

Band Model Parameters for the  $2.7\text{-}\mu\text{m}$  Bands of  
 $\text{H}_2\text{O}$  and  $\text{CO}_2$  in the 100 to  $3000^\circ\text{K}$   
Temperature Range

AD A 014248

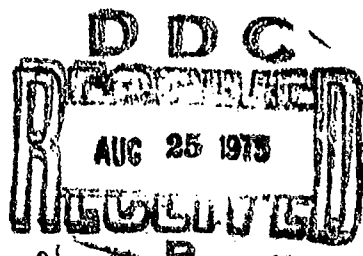
S. J. YOUNG  
Chemistry and Physics Laboratory  
Laboratory Operations  
The Aerospace Corporation  
El Segundo, Calif. 90245



31 July 1976

Interim Report

APPROVED FOR PUBLIC RELEASE:  
DISTRIBUTION UNLIMITED



Sponsored by

DEFENSE ADVANCED RESEARCH PROJECTS AGENCY  
1400 Wilson Blvd  
Arlington, Va. 22209

DARPA Order No. 2843

SPACE AND MISSILE SYSTEMS ORGANIZATION  
AIR FORCE SYSTEMS COMMAND  
Los Angeles Air Force Station  
Los Angeles, Calif. 90045

THE VIEWS AND CONCLUSIONS CONTAINED IN THIS DOCUMENT ARE THOSE  
OF THE AUTHORS AND SHOULD NOT BE INTERPRETED AS NECESSARILY  
REPRESENTING THE OFFICIAL POLICIES, EITHER EXPRESSED OR IMPLIED, OF  
THE DEFENSE ADVANCED RESEARCH PROJECTS AGENCY OR THE U.S.  
GOVERNMENT.

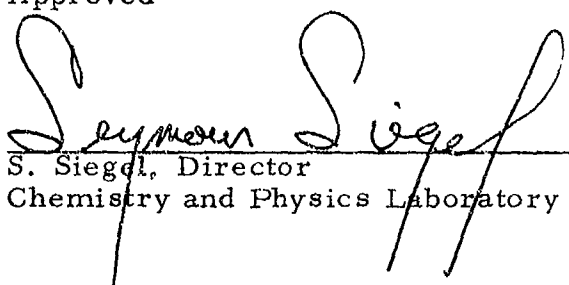
**BEST**

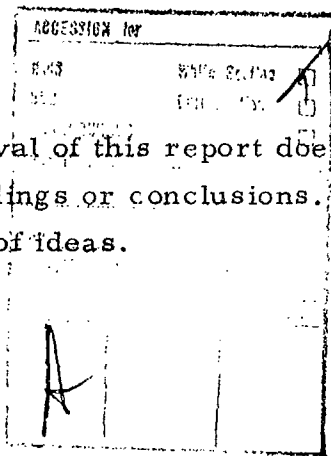
**AVAILABLE**

**COPY**

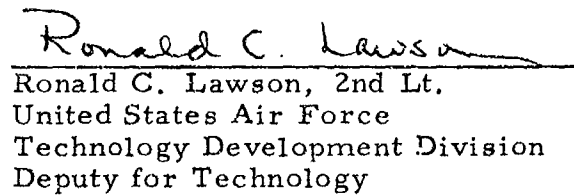
This research was supported by the Defense Advanced Research Projects Agency of the Department of Defense and was monitored by Space and Missile Systems Organization (SAMSO) under Contract No. F04701-75-C-0076.

Approved

  
S. Siegel, Director  
Chemistry and Physics Laboratory



Approval of this report does not constitute Air Force approval of the report's findings or conclusions. It is published only for the exchange and stimulation of ideas.

  
Ronald C. Lawson  
Ronald C. Lawson, 2nd Lt.  
United States Air Force  
Technology Development Division  
Deputy for Technology

## UNCLASSIFIED

SECURITY CLASSIFICATION OF THIS PAGE (When Data Entered)

micrometers

REPORT DOCUMENTATION PAGE		READ INSTRUCTIONS BEFORE COMPLETING FORM	
1. REPORT NUMBER <i>(18) SAMSO TR -75-209</i>	2. GOVT ACCESSION NO.	3. RECIPIENT'S CATALOG NUMBER	
4. TITLE (and Subtitle) BAND MODEL PARAMETERS FOR THE 2.7- BANDS OF H <sub>2</sub> O AND CO <sub>2</sub> IN THE 100 TO 3000 K TEMPERATURE RANGE		5. TYPE OF REPORT & PERIOD COVERED Interim	
6. AUTHORITY Stephen J. Young		7. PERFORMING ORG. REPORT NUMBER TR -0076(6970) -4	
8. CONTRACT OR GRANT NUMBER(s) F04701-75-C-0076		10. PROGRAM ELEMENT, PROJECT, TASK AREA & WORK UNIT NUMBERS	
9. PERFORMING ORGANIZATION NAME AND ADDRESS The Aerospace Corporation El Segundo, Calif. 90245		11. CONTROLLING OFFICE NAME AND ADDRESS Defense Advanced Research Projects Agency 1400 Wilson Blvd. Arlington, Va. 22209	
12. REPORT DATE 11/31 July 1975		13. NUMBER OF PAGES 57	
14. MONITORING AGENCY NAME & ADDRESS (if different from Controlling Office) Space and Missile Systems Organization Air Force Systems Command Los Angeles, Calif. 90045		15. SECURITY CLASS. (of this report) Unclassified	
16. DISTRIBUTION STATEMENT (of this Report) Approved for public release; distribution unlimited			
17. DISTRIBUTION STATEMENT (of the abstract entered in Block 20, if different from Report)			
18. SUPPLEMENTARY NOTES The views and conclusions contained in this document are those of the authors and should not be interpreted as necessarily representing the official policies, either expressed or implied, of The Defense Advanced Research Projects Agency or the U.S. Government.			
19. KEY WORDS (Continue on reverse side if necessary and identify by block number) Absorption by CO <sub>2</sub> Absorption by H <sub>2</sub> O Atmospheric Absorption			
20. ABSTRACT (Continue on reverse side if necessary and identify by block number) Sets of band model parameters for H <sub>2</sub> O and CO <sub>2</sub> in the 2.7- $\mu\text{m}$ spectral region, and consistent for the entire temperature range from near-ambient atmospheric temperatures ( $\sim 200^\circ\text{K}$ ) to gas combustion temperatures ( $\sim 2500^\circ\text{K}$ ), are constructed. These constructions are accomplished by joining together band model parameters derived from the AFCRL atmospheric absorption line data compilation (LINAVER parameters) and parameters tabulated in the NASA Handbook of Infrared Radiation from Combustion Gases (NASA parameters).			

## UNCLASSIFIED

SECURITY CLASSIFICATION OF THIS PAGE(When Data Entered)

## 19. KEY WORDS (Continued)

Band Model Parameters  
High-Temperature Absorption

## 20. ABSTRACT (Continued)

The former set adequately describes the low-temperature variation of the parameters but is inadequate for some high-temperature applications. The latter set is suitable for high-temperature applications but fails for some low-temperature cases. Examples of the deficiencies of these two sets are presented by comparison with experimental absorption and emission spectra for low- and high-temperature gas samples. The adequacy of the combined band model parameter set (COMB parameters) is demonstrated by comparison with the same experimental data. Criteria for and examples of the construction of the combined sets are given, and tabulations of the parameter sets are included in an Appendix. An example of the use of the new parameter sets is given by computation of the effective transmittance of the atmosphere for a hot H<sub>2</sub>O/CO<sub>2</sub> emission source viewed over a long atmospheric slant path.

UNCLASSIFIED

SECURITY CLASSIFICATION OF THIS PAGE(When Data Entered)

## CONTENTS

I.	INTRODUCTION . . . . .	3
II.	BAND MODEL PARAMETERS . . . . .	7
A.	Band Model Formulation . . . . .	7
B.	Band Model Parameters from Line Data (LINAIVE parameters) . . . . .	11
C.	NASA Parameters . . . . .	19
D.	Evaluation of Parameter Sets . . . . .	20
III.	COMBINED PARAMETER SETS . . . . .	33
A.	General Procedure . . . . .	33
B.	H <sub>2</sub> O Parameter Set (COMBH2O) . . . . .	34
C.	CO <sub>2</sub> Parameter Set (COMBCO2) . . . . .	37
IV.	ATMOSPHERIC TRANSMITTANCE CALCULATION . . . . .	41
APPENDIX: COMBH2O AND COMBCO2 PARAMETER SET LISTINGS . . . . .		47

## TABLES

1.	Line Broadening Parameters for H <sub>2</sub> O and CO <sub>2</sub> . . . . .	17
A1.	Listing of COMBH2O Band Model Parameter Set . . . . .	48
A2.	Listing of COMBCO2 Band Model Parameter Set . . . . .	52

## FIGURES

1.	Low-Temperature Transmission Spectra for CO <sub>2</sub> in the Band Center Region .....	22
2.	Low-Temperature Transmission Spectra for CO <sub>2</sub> in the Band Wing Region .....	24
3.	High-Temperature Emission Spectra for CO <sub>2</sub> .....	25
4.	Low-Temperature Transmission Spectra for H <sub>2</sub> O .....	27
5.	Low-Temperature Transmission Spectra for H <sub>2</sub> O in the Band Center Region .....	28
6.	Low-Temperature Transmission Spectra for H <sub>2</sub> O in the Band Wing Region .....	29
7.	High-Temperature Emission Spectra for H <sub>2</sub> O .....	31
8.	Variation of $\bar{k}$ (H <sub>2</sub> O) with Temperature for Selected Spectral Intervals .....	35
9.	Variation of $1/\delta_e$ (H <sub>2</sub> O) with Temperature for Selected Spectral Intervals .....	36
10.	Variation of $\bar{k}$ (CO <sub>2</sub> ) with Temperature for Selected Spectral Intervals .....	38
11.	Variation of $1/\delta_e$ (CO <sub>2</sub> ) with Temperature for Selected Spectral Intervals .....	39
12.	Source and Transmitted Radiance Spectra for Atmospheric Slant Path .....	43
13.	Transmittance Spectra for Atmospheric Slant Path .....	44
14.	Effective Transmittance Spectra for Atmospheric Slant Path .....	45

## I. INTRODUCTION

In a previous report,<sup>1</sup> band model techniques were applied to the problem of computing the effective transmittance of the atmosphere for radiation arising from hot gaseous H<sub>2</sub>O and CO<sub>2</sub> emission sources. Effects of line correlation between the emission spectra and atmospheric absorption spectra were accounted for by treatment of the entire optical path consisting of the atmospheric slant path plus the line-of-sight continuation through the source as a single, highly inhomogeneous radiating and absorbing entity. Approximations for handling the large degree of inhomogeneity caused by pressure, temperature, and species concentration gradients along such an optical path were discussed.

The single most important variable that affects the degree of inhomogeneity of the path is the temperature distribution along the path. Through the atmospheric portion of the total path, the temperature variations are slight, and for many applications, the atmosphere can be considered as isothermal. In the transition region between the atmospheric portion and the source portion of the path, and within the source portion itself, large temperature gradients can exist. The effect of these temperature gradients is introduced into the band model calculations through the temperature variation of the fundamental band model parameters that describe the absorption effects of all the spectral lines in a small spectral interval  $\Delta\nu$ .

In the previous work, two sets of band model parameters were employed. The set designated LINAVE was generated from the line

---

<sup>1</sup>S. J. Young, Band Model Calculations of Atmospheric Transmittance for Hot Gas Line Emission Sources, TR-0075(5647)-1, The Aerospace Corp., El Segundo, Calif. (31 December 1974).

strength and width data of the Air Force Cambridge Research Laboratories (AFCRL) line atlas.<sup>2</sup> The parameter set designated GD\* was taken from the NASA Handbook of Infrared Radiation from Combustion Gases.<sup>3</sup> The former set was expected to be reasonably accurate for low temperatures since the AFCRL line atlas was compiled primarily for atmospheric applications. Its use at higher temperatures was demonstrated to be inadequate in the 2.7- $\mu\text{m}$  band wing regions. The latter set, since it was constructed for high-temperature problems, was expected to be adequate for temperatures above about 1000°K but to be of questionable utility for low temperatures. If the problem of atmospheric transmittance could be treated in a manner in which the source emission and atmospheric absorption were decoupled processes, these existing parameter sets would be sufficient to handle transmittance computations. Since the correct account of line correlation requires the entire optical path to be treated as a single entity, however, a single set of band model parameters, applicable to the entire temperature range from atmospheric temperatures (at least as low as 200°K) to combustion gas temperatures (at least as high as 2500°K), is required.

The work described in this report is concerned with the construction of band model parameter sets for the 2.7- $\mu\text{m}$  bands of  $\text{H}_2\text{O}$  and  $\text{CO}_2$  that

\*These parameters were generated by workers at General Dynamics, hence the designation GD. Most people, however, refer to these data as the NASA parameters. The latter designation will be used in the remainder of this report.

<sup>2</sup>R. A. McClatchey, W. S. Benedict, S. A. Clough, D. E. Burch, R. F. Calfe, K. Fox, L. S. Rothman, and J. S. Garing, AFCRL Atmospheric Absorption Line Parameters Compilation, AFCRL-TR-73-006, Air Force Cambridge Research Laboratories, Mass. (25 January 1973).

<sup>3</sup>C. B. Ludwig, W. Malkmus, J. E. Reardon, and J. A. L. Thompson, Handbook of Infrared Radiation from Combustion Gases, eds. R. Goulard and J. A. L. Thompson, NASA SP-3080, Marshall Space Flight Center, Huntsville, Ala. (1973).

are internally consistent for the temperature range from 100 to 3000°K. Section II of this report discusses the generation of the LINAVE and NASA parameter sets and gives examples of their deficiencies. The combining of these two parameter sets to give consistent sets for H<sub>2</sub>O and CO<sub>2</sub> is done in Sect. III. An example of their use in an atmospheric transmittance problem is given in Sect. IV.

## II. BAND MODEL PARAMETERS

### A. BAND MODEL FORMULATION

The statistical band model formulation\* for absorption by a random array of pressure-broadened Lorentz lines depends on the specification of three fundamental band model parameters. The mean absorption coefficient  $\bar{k}$  describes the strength of absorption effected by all the lines in a spectral interval  $\Delta\nu$ , the mean line-spacing parameter  $\delta_e$  measures the effective average distance between adjacent lines in  $\Delta\nu$ , and  $\bar{\gamma}$  gives the mean line width of the lines in  $\Delta\nu$ . For most applications,  $\delta_e$  and  $\bar{\gamma}$  do not need to be known individually, and the mean line width to spacing parameter

$$\beta = \frac{2\pi \bar{\gamma}}{\delta_e} \quad (1)$$

along with  $\bar{k}$  suffices to specify the absorption characteristic of  $\Delta\nu$ . In general, the parameters  $\bar{k}$  and  $\delta_e$  are functions of spectral position and temperature while  $\bar{\gamma}$  depends additionally on the pressure and species composition of the absorbing gas.

For a homogeneous optical path and a single active gas species, the mean transmittance in  $\Delta\nu$  is

$$\bar{\tau} = \exp \left( - \frac{W}{\delta} \right) \quad (2)$$

\* More accurately, we mean the approximation to the statistical band model in which the number of lines in an interval  $\Delta\nu$  is assumed to be infinite and for which the absorption by each line whose center occurs in  $\Delta\nu$  is complete within  $\Delta\nu$ .

where  $\bar{W}$  is the mean equivalent width of all the lines in  $\Delta\nu$  and

$$\delta = \frac{\Delta\nu}{N} \quad (3)$$

is the mean line-spacing parameter. The number of lines in  $\Delta\nu$  is  $N$ . In terms of band model parameters,

$$\frac{\bar{W}}{\delta} = \beta f(x) \quad (4)$$

where

$$x = \frac{k u}{\beta} \quad (5)$$

is the dimensionless optical depth parameter. The optical depth  $u$  is the product of the total gas pressure  $p$ , the mole fraction of the active gas  $c$ , and the geometric path length  $L$ :

$$u = p c L \quad . \quad (6)$$

The curve-of-growth function  $f(x)$  depends on the line strength distribution function assumed for the lines in  $\Delta\nu$ . For equal intensity lines,

$$f(x) = L(x) \quad (7)$$

where  $L(x)$  is the Ladenburg-Reiche function. For an exponential distribution of line strengths,

$$f(x) = \frac{x}{\sqrt{1 + \frac{\pi x}{2}}} \quad (8)$$

while for the exponential-tailed inverse distribution,<sup>\* 4</sup>

$$f(x) = \frac{1}{\pi} \left[ \sqrt{1 + 2\pi x} - 1 \right]. \quad (9)$$

These curve-of-growth functions are all defined so that  $f(x) \rightarrow x$  for small  $x$  and  $f(x) \rightarrow (2x/\pi)^{1/2}$  for large  $x$ . In this way, the same band model parameters are appropriate for all three distribution functions.

For application of the statistical band model to inhomogeneous optical paths, approximations must be introduced to account for pressure, species concentration, and temperature gradients along the line of sight. In both the Curtis-Godson (CG) and Lindquist-Simmons (LS) approximations, this account is made by the employment of path-averaged values of the band model parameters. For a path extending from the geometric position  $s = 0$  to the general position  $s$  along the line of sight, the appropriate path averages are

$$\bar{k}_e(s) = \frac{1}{u(s)} \int_0^s c(s') p(s') \bar{k}(s') ds' \quad (10)$$

and

$$\beta_e(s) = \frac{1}{u(s) \bar{k}_e(s)} \int_0^s c(s') p(s') \bar{k}(s') \beta(s') ds' \quad (11)$$

---

<sup>\*</sup>The exponential-tailed inverse line strength distribution was invented by Malkmus (Ref. 4) as an approximation to the purely inverse line strength distribution function. The resulting curve of growth function [Eq. (9)] is substantially simpler in form than that for the inverse distribution.

<sup>4</sup>W. Malkmus, J. Opt. Soc. Am. 57, 323 (1967).

where

$$u(s) = \int_0^s c(s') p(s') ds' . \quad (12)$$

In the CG approximation,  $\bar{k}_e$  and  $\beta_e$  are used in place of  $\bar{k}$  and  $\delta$ , respectively, in the equations for a homogeneous optical path. In the LS approximation, these path-averaged parameters are used to define the quantities

$$x_e(s) = \frac{\bar{k}_e(s) u(s)}{\beta_e(s)} \quad (13)$$

and

$$p(s) = \frac{\beta(s)}{\beta_e(s)} , \quad (14)$$

which are used in turn to give the transmittance derivative function

$$y(s) = y[x_e(s), p(s)] . \quad (15)$$

The functional form of  $y(x, p)$  with  $x$  and  $p$  depends on the line shape and the line strength distribution employed. The transmittance in the LS approximation is then given by Eq. (2) where  $\bar{W}/\delta$  is given by

$$\frac{\bar{W}(s)}{\delta} = \int_0^s c(s') p(s') \bar{k}(s') y(s') ds' . \quad (16)$$

A more detailed account of these approximations is given elsewhere.<sup>1, 5</sup>

---

<sup>5</sup>S. J. Young, Band Model Formulation for Inhomogeneous Optical Paths, TR-0075(5647)-4, The Aerospace Corp., El Segundo, Calif. (19 December 1974).

The important feature of both of these approximations is that the parameters  $\bar{k}$ ,  $\delta_e$ , and  $\bar{\gamma}$  need to be known for the entire range of variation of the thermodynamic properties of the path. For the highly inhomogeneous optical path consisting of a long atmospheric slant path, plus a line-of-sight continuation through a hot-gas missile exhaust plume, for example, the path temperature  $T(s)$  can range from as low as  $\sim 190^{\circ}\text{K}$  to as high as  $\sim 3000^{\circ}\text{K}$ . Thus, both  $\bar{k}$  and  $\delta_e$  must be known for this same range of temperature variation in order to compute the path averages of Eqs. (10) and (11). It is this variation of  $\bar{k}$  and  $\delta_e$  over large temperature ranges that is of primary concern. The variation of  $\bar{\gamma}$  with temperature and pressure is adequately described by variations of the form  $\bar{\gamma} \sim p/T^n$  where  $n$  is of the order of unity. Thus,  $\bar{\gamma}$  will vary about an order of magnitude between the temperature limits indicated above. For this same temperature range, however,  $\bar{k}$  and  $\delta_e$  may vary by several orders of magnitude.

#### B. BAND MODEL PARAMETERS FROM LINE DATA (LINA VE PARAMETERS)

If the line strength  $S(i)$  and line width  $\gamma(i)$  of all the important lines in  $\Delta\nu$  are known, the band model parameters  $\bar{k}$ ,  $\delta_e$ , and  $\bar{\gamma}$  can be derived in terms of  $S(i)$  and  $\gamma(i)$ . The procedure is to force an exact agreement between the weak and strong limits of absorption for the statistical band model described in terms of the line parameters and the model described in terms of the band model parameters. For the former description, we write the mean equivalent width for all the lines in  $\Delta\nu$  as

$$\frac{\bar{W}}{\delta} = \frac{1}{\delta} \left\{ \frac{1}{N} \sum_{i=1}^N W(i) \right\} = \frac{1}{\Delta\nu} \sum_{i=1}^N W(i) \quad (17)$$

where  $W(i)$  is the equivalent width of the  $i^{\text{th}}$  line. For a Lorentz line (and homogeneous path),

$$W(i) = 2\pi \gamma(i) L(x) \quad (18)$$

where

$$x = \frac{S(i) u}{2\pi \gamma(i)} . \quad (19)$$

The description in terms of band model parameters is given by Eqs. (1), (4), and (5). Repeating for convenience,

$$\frac{\bar{W}}{\delta} = \beta f(x) \quad (20)$$

$$\beta = \frac{2\pi Y}{\delta_e} \quad (21)$$

and

$$x = \frac{\bar{k} u}{\beta} . \quad (22)$$

In the limit of weak absorption (that is, as  $x \rightarrow 0$ ), Eqs. (17) through (19) give

$$\frac{\bar{W}}{\delta} \approx \frac{u}{\Delta v} \sum_{i=1}^N S(i)$$

while Eqs. (20) through (22) yield

$$\frac{\bar{W}}{\delta} \simeq \bar{k} u .$$

Equation of these two weak-limit expressions for  $\bar{W}/\delta$  yields the solution for  $\bar{k}$

$$\bar{k} = \frac{1}{\Delta \nu} \sum_{i=1}^N S(i) . \quad (23)$$

For strong absorption (as  $x \rightarrow \infty$ ), Eqs. (17) through (19), give

$$\frac{\bar{W}}{\delta} \simeq \frac{2 \sqrt{u}}{\Delta \nu} \sum_{i=1}^N \sqrt{S(i) \gamma(i)}$$

while Eqs. (20) through (22) yield

$$\frac{\bar{W}}{\delta} \simeq 2 \sqrt{u} \sqrt{\frac{\bar{k} \gamma}{\delta_e}} .$$

Equation of these two strong-limit forms for  $\bar{W}/\delta$  yields the solution for  $\delta_e$

$$\frac{1}{\delta_e} = \frac{1}{\bar{k} \gamma} \left[ \frac{1}{\Delta \nu} \sum_{i=1}^N \sqrt{S(i) \gamma(i)} \right]^2 . \quad (24)$$

The forced agreement for weak and strong absorption supplys two conditions for the determination of the three band model parameters. In order to complete the determination, we simply define  $\bar{\gamma}$  to be

$$\bar{\gamma} = \frac{1}{N} \sum_{i=1}^N \gamma(i) . \quad (25)$$

Equations (23), (24), and (25) define the band model parameters  $\bar{k}$ ,  $\delta_e$ , and  $\bar{\gamma}$  in terms of the line data  $S(i)$  and  $\gamma(i)$ ,  $i = 1, 2, \dots, N$ .

These defining equations have been used to construct band model parameter sets for both  $H_2O$  and  $CO_2$ . The line strength and width data were derived from the comprehensive line atlas compiled by AFCRL.\* This compilation provides line data for each of over 120,000 lines for seven atmospheric absorbing gas species including  $H_2O$  and  $CO_2$ . The data given for each line include the line position  $\nu(cm^{-1})$ , the line strength  $S_a(cm^{-1}/molecule\cdot cm^{-2}$  at  $296^\circ K$ ), the line half-width  $\gamma_a(cm^{-1}$  for air-broadening at  $296^\circ K$  and 1 atm pressure), and the energy of the lower level of the transition  $E(cm^{-1})$ . The line strength for the  $i^{th}$  line at temperature  $T$  is computed from the value  $S_a$  given at the standard temperature  $T_a = 296^\circ K$  by

$$S_i(T) = C(T) S_a \frac{Q_R(T_a) Q_V(T_a)}{Q_R(T) Q_V(T)} \left[ \frac{1 - e^{-\nu(i)/kT}}{1 - e^{-\nu(i)/kT_a}} \right] \\ \times \exp \left[ -\frac{E(i)}{k} \left( \frac{1}{T} - \frac{1}{T_a} \right) \right] . \quad (26)$$

The factors  $Q_R$  and  $Q_V$  are the rotational and vibrational partition functions, respectively, of the molecule. The exponential term accounts for the

---

\*The compilation version dated 4 Feb 1975 by AFCRL was used in this work.

Boltzmann distribution population of molecules in the energy level  $E(i)$ , and the term in brackets accounts for stimulated emission. The ratio of rotational partition functions is approximated by

$$\frac{Q_R(T_a)}{Q_R(T)} \approx \left( \frac{T_a}{T} \right)^m \quad (27)$$

where  $m = 1.5$  for  $H_2O$  ( $H_2O$  is assumed to be a nearly symmetric-top molecule) and  $m = 1$  for  $CO_2$ . The molecular vibrational partition function is assumed to be the product of simple harmonic oscillator partition functions for each vibrational mode of the molecule:

$$Q_V(T) = \left[ 1 - e^{-\nu_1/kT} \right]^{-d_1} \left[ 1 - e^{-\nu_2/kT} \right]^{-d_2} \left[ 1 - e^{-\nu_3/kT} \right]^{-d_3} \quad (28)$$

where  $\nu_1$ ,  $\nu_2$ , and  $\nu_3$  are the fundamental oscillatory frequencies of the molecule and  $d_1$ ,  $d_2$ , and  $d_3$  are the degeneracies associated with these modes of vibration. For  $CO_2$ ,  $\nu_1 = 1388.17 \text{ cm}^{-1}$ ,  $\nu_2 = 667.40 \text{ cm}^{-1}$ , and  $\nu_3 = 2349.16 \text{ cm}^{-1}$ . For  $H_2O$ ,  $\nu_1 = 3657.0 \text{ cm}^{-1}$ ,  $\nu_2 = 1594.7 \text{ cm}^{-1}$ , and  $\nu_3 = 3755.7 \text{ cm}^{-1}$ . The degeneracies for all modes of both  $CO_2$  and  $H_2O$  are unity, except for the doubly degenerate bending mode  $\nu_2$  in the linear  $CO_2$  molecule, for which  $d_2 = 2$ . The value of  $1/k$  is  $1.439 \text{ cm}^{-1}\text{K}^{-1}$ .

The factor  $C(T)$  of Eq. (26) converts the line strength from the AFCRL unit of  $\text{cm}^{-1}/\text{molecule}\cdot\text{cm}^{-2}$  to the unit  $\text{cm}^{-2}/\text{atm}$  and is

$$C(T) = 2.480 \times 10^{19} \frac{296^\circ\text{K}}{T} \frac{\text{molecules}}{\text{atm cm}^3} \quad . \quad (29)$$

Equations (26) through (29) give the required line strengths  $S(i)$  to be used in Eq. (23) to calculate  $\bar{k}$  for any spectral interval  $\Delta\nu$  and at any temperature  $T$ .

The line-broadening parameters of the AFCRL atlas are the broadening parameters appropriate to foreign gas broadening by air at 296°K. The mean line width parameter  $\bar{\gamma}_a$  computed according to Eq. (25) will reflect broadening for these same conditions. Specification of the line-broadening parameter in terms of air broadening would be suitable if only atmospheric absorption paths were considered. In a hot, combustion gas environment, however, this description is not quite as appropriate. Now, account has to be made of broadening by  $H_2O$  and  $CO_2$  as well. In addition, even if the concentrations of  $H_2O$  and  $CO_2$  are small, the remaining gas is usually not air but  $N_2$  (the  $O_2$  having been used in the combustion process).

An adequate description of line pressure broadening for the species  $s$  is given by

$$\bar{\gamma}_s(p, T) = p \left[ c_s (\bar{\gamma}_s^*)_0 \left( \frac{273}{T} \right)^{n_s^*} + \sum_f \left\{ c_f \left( \bar{\gamma}_s^f \right)_0 \left( \frac{273}{T} \right)^{n_s^f} \right\} \right] . \quad (30)$$

The summation term accounts for foreign gas broadening ( $f \neq s$ ) and non-resonant self-broadening ( $f = s$ ) contributions to the line width. The first term accounts for resonant self-broadening effects that occur primarily for  $H_2O$ . The  $c$  terms are the mole fractions of the gas constituents, and the  $(\bar{\gamma})_0$  parameters are the broadening parameters for standard temperature (273°K) and pressure (1 atm) conditions. The exponents,  $n$ , determine the degree of temperature variation. Nominally,  $n \sim 1/2$  and  $n^* \sim 1$ . Values of  $(\bar{\gamma})_0$  and exponent parameters recommended in the NASA Handbook<sup>3</sup> are given in Table 1.

Table 1. Line-Broadening Parameters for H<sub>2</sub>O and CO<sub>2</sub><sup>a</sup>

Molecule (s)	Broadener (f)	( $\bar{\gamma}_s^*$ ) <sub>0</sub> (cm <sup>-1</sup> /atm)	n <sub>s</sub> <sup>*</sup>	( $\bar{\gamma}_s^f$ ) <sub>0</sub> (cm <sup>-1</sup> /atm)	n <sub>s</sub> <sup>f</sup>
H <sub>2</sub> O	H <sub>2</sub> O	0.44	1.0	(0.09)	0.5
	CO <sub>2</sub>		0.12		0.5
	N <sub>2</sub>		0.09		0.5
	O <sub>2</sub>		0.04		0.5
CO <sub>2</sub>		0.01	1.0	0.09	0.5
	H <sub>2</sub> O			(0.07)	0.5
	N <sub>2</sub>		0.07		0.5
	O <sub>2</sub>		0.055		0.5

<sup>a</sup>Data taken from Ref. 3. Values in parentheses are estimates.

Of the three parameters  $(\bar{\gamma}_s^*)_0$ ,  $(\bar{\gamma}_s^f)_0$ , and  $(\bar{\gamma}_s^s)_0$ , the latter has been selected here as the fundamental line-broadening parameter; that is, the value for nonresonant self-broadening at STP. If  $\bar{\gamma}_a$  is the mean width parameter for air broadening at 1 atm and 296°K computed according to Eq. (25), then Eq. (30) and Table 1 can be used to derive

$$\bar{\gamma}_0 \equiv (\bar{\gamma}_s^s)_0 = c \bar{\gamma}_a \quad (31)$$

where  $c = 1.186$  for  $s = H_2O$  and  $c = 1.405$  for  $s = CO_2$ . The actual mean line width  $\bar{\gamma}$  can be computed from the thermodynamic conditions of the optical path and  $\bar{\gamma}_0$  by means of Eq. (30) written in the form

$$\bar{\gamma} = \bar{\gamma}_0 P \left[ c_s \alpha_s^* \left( \frac{273}{T} \right)^{n_s^*} + \sum_f c_f \alpha_s^f \left( \frac{273}{T} \right)^{n_s^f} \right] \quad (32)$$

where the  $\alpha$  coefficients are the ratios of the  $(\bar{\gamma})_0$  coefficients to  $(\bar{\gamma}_s^s)_0$  and are obtained from Table 1 ( $\alpha_s^s = 1$ ). Note that none of these considerations on the line width parameters affect the evaluation of  $\delta_e$  by Eq. (24) since any conversion factors applied to  $\gamma(i)$  cancel.

For the present work, two sets of line-averaged band model parameters were generated. The set for  $H_2O$  (LINAVERH2O) contains  $\bar{k}(v, T)$ ,  $1/\delta_e(v, T)$ , and  $\bar{\gamma}_0(v)$  for  $v = 2500$  to  $4500 \text{ cm}^{-1}$  by steps of  $25 \text{ cm}^{-1}$  with  $\Delta v = 25 \text{ cm}^{-1}$  and for the 14 values of temperature  $T = 100, 150, 200, 250, 300, 350, 400, 500, 750, 1000, 1500, 2000, 2500$ , and  $3000^\circ K$ . The set for  $CO_2$  (LINAVERCO2) contains the same parameters for the same temperatures but for  $v = 3080$  to  $3860 \text{ cm}^{-1}$  by steps of  $5 \text{ cm}^{-1}$  and  $\Delta v = 5 \text{ cm}^{-1}$ . In all cases,  $\bar{k}$  has the unit  $\text{cm}^{-1}/\text{atm}$ ,  $\delta_e$  has the unit  $\text{cm}^{-1}$ , and  $\bar{\gamma}_0$  has the unit  $\text{cm}^{-1}/\text{atm}$  for nonresonant self-broadening at STP.

### C. NASA PARAMETERS

Sets of band model parameters generated by General Dynamics and intended primarily for use in high-temperature combustion gas applications have been in existence for several years. The most recent publication of these parameter sets is given by Ludwig et al. in the NASA Handbook.<sup>3</sup>

The data for CO<sub>2</sub> are the result of theoretical calculations based on the known quantum mechanical properties of linear triatomic molecules.<sup>6</sup> The approach is similar to that presented in the preceding section. Line strengths were computed theoretically and averaged to yield  $\bar{k}$  and  $\delta_e$ . For the 2.7-μm band region,  $\bar{k}$  values are given for the temperature range from 300 to 3000°K but  $\delta_e$  is given only up to 1800°K. The  $\delta_e$  data for temperatures between 1800 and 3000°K, however, can be obtained from the report by Huffaker and Dash.<sup>7</sup> With the data from these two sources, a CO<sub>2</sub> band model parameter set (NASACO2) was constructed\* for  $\nu = 3000$  to  $3770 \text{ cm}^{-1}$  by  $5\text{-cm}^{-1}$  steps and for the seven temperatures  $T = 300, 600, 1200, 1500, 1800, 2400$ , and  $3000^\circ\text{K}$ . The spectral resolution of the data appears to be

\*When required, linear interpolations with respect to  $\nu$  and semilogarithmic interpolations with respect to  $T$  were used. The  $\delta_e$  data at  $\nu = 3080 \text{ cm}^{-1}$  was assumed to prevail between 3000 and  $3080 \text{ cm}^{-1}$ . The spurious temperature variation at  $T = 1200^\circ\text{K}$  for  $3110 \leq \nu \leq 3150 \text{ cm}^{-1}$  was removed from the  $\bar{k}$  data by defining these values to be zero. An order-of-magnitude error in the  $1200^\circ\text{K}$  data at  $\nu = 3660 \text{ cm}^{-1}$  was corrected in the  $\bar{k}$  data by using  $\bar{k} = 0.3471 \text{ cm}^{-1}$  rather than the listed value of  $0.03471 \text{ cm}^{-1}$ . This correction also affects the values on either side of  $3660 \text{ cm}^{-1}$ ; the  $\bar{k}$  value at  $3655 \text{ cm}^{-1}$  was changed from  $0.1877$  to  $0.3439 \text{ cm}^{-1}$  and the value at  $3665 \text{ cm}^{-1}$  from  $0.2197$  to  $0.3759 \text{ cm}^{-1}$ . An apparent order-of-magnitude error in  $\bar{k}$  for  $T = 300^\circ\text{K}$  at  $\nu = 3540 \text{ cm}^{-1}$  was corrected by replacing the value  $4.889 \times 10^{-2}$  by  $4.889 \times 10^{-3} \text{ cm}^{-1}$ .

<sup>6</sup>W. Malkmus, J. Opt. Soc. Am. **54**, 751 (1964).

<sup>7</sup>R. M. Huffaker and M. J. Dash, A General Program for the Calculation of Radiation from an Inhomogeneous, Nonisobaric, Nonisothermal Rocket Exhaust Plume, NASA TM X-53622, Marshall Space Flight Center, Huntsville, Ala. (19 June 1967).

$\Delta\nu \approx 5 \text{ cm}^{-1}$ . The NASA unit for  $\bar{k}$  is  $\text{cm}^{-1}$  at STP and was converted to the unit  $\text{cm}^{-1}/\text{atm}$  by multiplication by  $273/T$ . The  $\bar{\gamma}_0$  coefficient is taken as a constant for all  $\Delta\nu$  intervals with the value (from Table 1)  $\bar{\gamma}_0 = 0.09 \text{ cm}^{-1}/\text{atm}$ .

The NASA parameters for  $\text{H}_2\text{O}$  were derived for the most part from experimental measurements.<sup>8</sup> Because of the nonlinearity of  $\text{H}_2\text{O}$ , exact theoretical calculation of band model parameters is extremely complicated and difficult, particularly at high temperatures. The bulk of the  $\text{H}_2\text{O}$  data above  $\sim 1200^\circ\text{K}$  were obtained in a consistent manner from emission-absorption measurements made on very long strip-burner  $\text{H}_2/\text{O}_2$  flames. Data below  $\sim 1200^\circ\text{K}$  are based on extrapolations from these high-temperature data and on the analysis of published low-temperature  $\text{H}_2\text{O}$  spectra. For the  $2.7\text{-}\mu\text{m}$  region,  $\bar{k}$  values are given for the temperature range from 300 to  $3000^\circ\text{K}$ , but  $\delta_e$  is given only down to  $600^\circ\text{K}$ . With these data, an  $\text{H}_2\text{O}$  band model parameter set (NASAH<sub>2</sub>O) was constructed between  $\nu = 2500$  and  $4500 \text{ cm}^{-1}$  by  $25\text{-cm}^{-1}$  steps at the seven temperatures  $T = 300, 600, 1000, 1500, 2000, 2500$ , and  $3000^\circ\text{K}$ . The spectral resolution of the data is  $\Delta\nu = 25 \text{ cm}^{-1}$ . The  $300^\circ\text{K}$  values of  $\delta_e$  at each wave number was obtained from a semilogarithmic extrapolation from the  $600$  and  $1200^\circ\text{K}$  data. Again, the unit of  $\bar{k}$  was converted from  $\text{cm}^{-1}$  at STP to  $\text{cm}^{-1}/\text{atm}$ , and  $\bar{\gamma}_0$  was taken as (Table 1)  $\bar{\gamma}_0 = 0.09 \text{ cm}^{-1}/\text{atm}$  for all  $\nu$ .

#### D. EVALUATION OF PARAMETER SETS

The AFCRL line atlas was compiled primarily for use in atmospheric transmittance problems. As a result, only those lines that are likely to be important near ambient atmospheric temperatures (say less than  $\sim 300^\circ\text{K}$ ) are specifically included. For most absorbing gases, these lines are absorption lines whose transition originates (in absorption) from the  $\nu = 0$  vibrational level of the ground electronic state of the molecule. For high-temperature problems, transitions originating from  $\nu \geq 1$  (hot bands) are likely to be important. Although many lines for which  $\nu \geq 1$  are included

---

<sup>8</sup>C. B. Ludwig, App. Opt. **10**, 1057 (1971).

in the AFCRL atlas, it can be anticipated that the LINAVE band model parameters derived from the atlas data may not be adequate for temperatures much above 300°K.

Conversely, the NASA parameters were generated specifically for high-temperature applications. Here, the problem is that the parameters are not particularly useful for low-temperature problems. Indeed, neither the set for CO<sub>2</sub> nor H<sub>2</sub>O give any data for T < 300°K, the region of most importance for atmospheric application.

The deficiencies of both the LINAVE and NASA parameters have been investigated quantitatively by comparing absorption spectra computed through the use of the parameters with high-quality experimental measurements made for homogeneous paths. Comparisons were made for both CO<sub>2</sub> and H<sub>2</sub>O and for both room-temperature and hot-gas conditions. The curve-of-growth function for the exponential-tailed inverse line strength distribution was used in the calculations.

#### 1. CO<sub>2</sub> AT 296°K

Burch et al.<sup>9</sup> have made high-resolution measurements of the absorption spectra of CO<sub>2</sub> at 296°K for a wide variety of optical thickness, partial pressure of CO<sub>2</sub>, and total pressure (with N<sub>2</sub> as the foreign gas). For most of the sample experimental cases, extensive tables are given from which the integrated absorptance between any two wave numbers can be calculated. In Fig. 1, the solid curves are the  $\bar{\tau}$  result for their sample no. 9 for which p = 0.00763 atm, c = 1.00, and L = 237 m. The optical depth is u = 181 atm cm. The curve was constructed for  $\Delta\nu = 5 \text{ cm}^{-1}$  and extends through the band center region from 3450 to 3775 cm<sup>-1</sup>. Figure 1(a) shows the comparison of the experimental spectrum with the spectrum computed with the

<sup>9</sup>D. E. Burch, D. A. Gryvnak, and R. R. Patty, Absorption by CO<sub>2</sub> Between 3100 and 4100 cm<sup>-1</sup> (2.44-3.22 Microns), U-4132, Aeronomutronic Div., Philco-Ford Corp., Newport Beach, Calif. (30 April 1968).

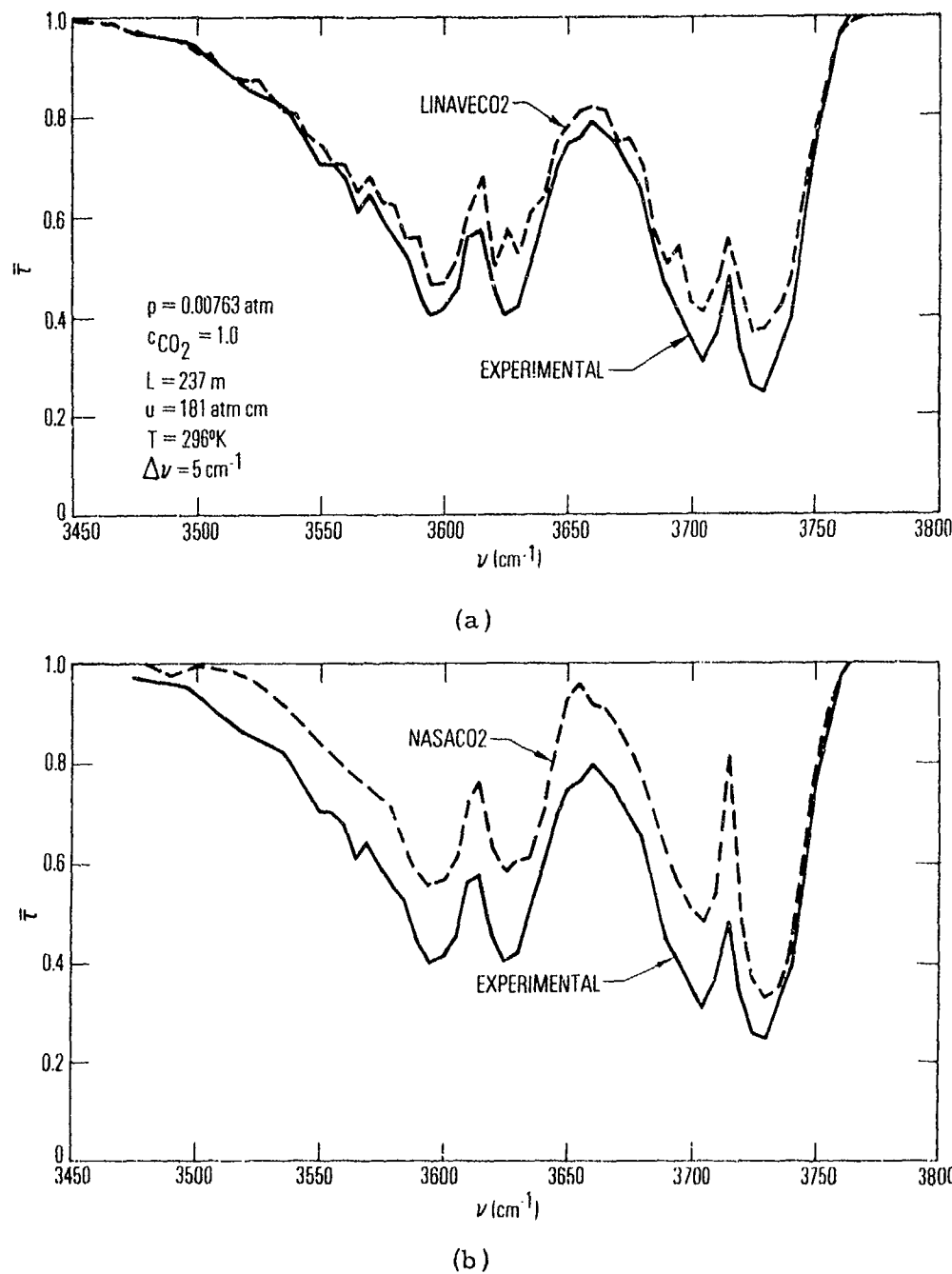


Fig. 1. Low-Temperature Transmission Spectra for  $\text{CO}_2$  in the Band Center Region. The LINAVECO<sub>2</sub> (a) and the NASACO<sub>2</sub> (b) curves show spectra computed with the indicated band model parameter set. The EXPERIMENTAL curve is derived from the tables of Ref. 9 for sample no. 9 and for  $\Delta\nu = 5 \text{ cm}^{-1}$ .

LINAVECO<sub>2</sub> parameters while Fig. 1(b) shows the comparison with the result obtained with the NASACO<sub>2</sub> parameters. Both of the parameter sets give results that underestimate the degree of absorption displayed by the experimental results. The LINAVECO<sub>2</sub> set, though, gives results that are in adequate agreement with the experimental spectrum. The underestimation of the absorptance in both cases may be the result of using a statistical rather than a regular line-spacing band model for CO<sub>2</sub> at low temperatures.

A similar comparison was made in the far wing region between 3100 and 3500 cm<sup>-1</sup>. Here, a much more strongly absorbing sample was chosen so that the absorptance would be measurable. The solid curves of Fig. 2 are the experimental results for sample no. 1 for which  $p = 2.5 \text{ atm}$ ,  $c = 1.00$ , and  $L = 933 \text{ m}$ . The optical thickness is  $u = 2.33 \times 10^5 \text{ atm cm}$  and again,  $\Delta\nu = 5 \text{ cm}^{-1}$ . The NASACO<sub>2</sub> values for  $\bar{k}$  are zero at 300°K for  $\nu \leq 3280 \text{ cm}^{-1}$ , and consequently, no amount of absorption is effected in the band wing. The LINAVE parameters yield an absorption spectrum that is in adequate agreement with the experimental spectrum.

## 2. CO<sub>2</sub> AT 1200°K

A high-temperature emission comparison was made between calculated emissivity spectra and an experimental spectrum of Burch and Gryvnak.<sup>10</sup> The experimental conditions were:  $p = 0.997 \text{ atm}$ ,  $c = 1.00$ ,  $L = 7.75 \text{ cm}$ , and  $T = 1200^\circ\text{K}$ . The optical thickness is  $u = 7.73 \text{ atm cm}$  and  $\Delta\nu \approx 7 \text{ cm}^{-1}$ . The comparison is shown in Fig. 3. Even at this high temperature, the result computed with the LINAVECO<sub>2</sub> parameters is in good agreement with the experimental result above  $\nu \approx 3550 \text{ cm}^{-1}$ . In the wing region below 3500 cm<sup>-1</sup>, however, the LINAVECO<sub>2</sub> parameters seriously underestimate the degree of emission and, below 3450 cm<sup>-1</sup>, predict no emission at all. The NASACO<sub>2</sub>

---

<sup>10</sup>D. E. Burch and D. A. Gryvnak, Infrared Radiation Emitted by Hot Gases and Its Transmission Through Synthetic Atmospheres, U-1929, Aeronutronic Div., Philco-Ford Corp., Newport Beach, Calif. (31 October 1962).

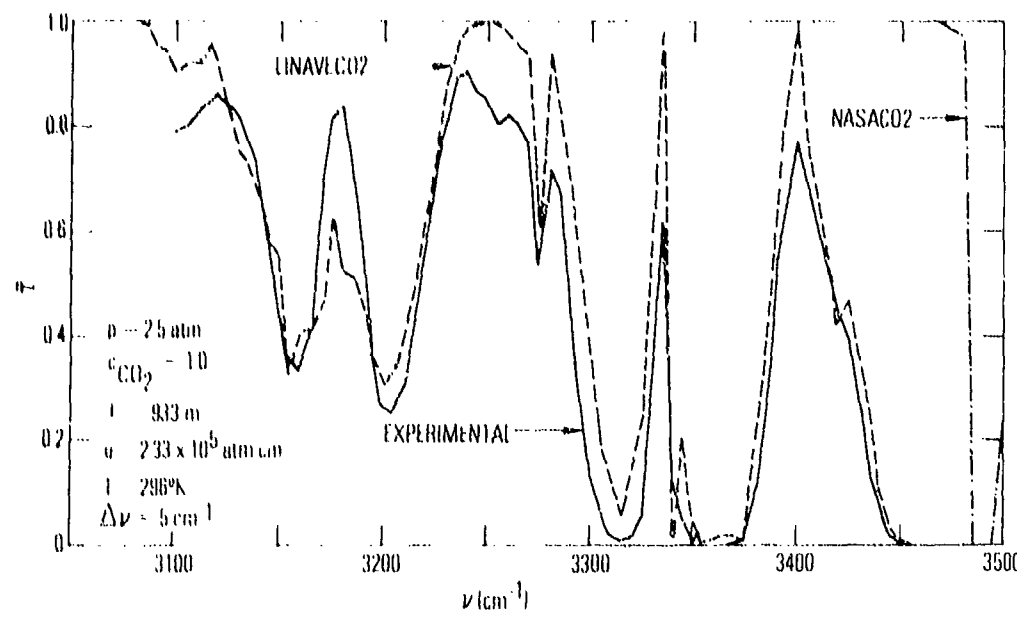
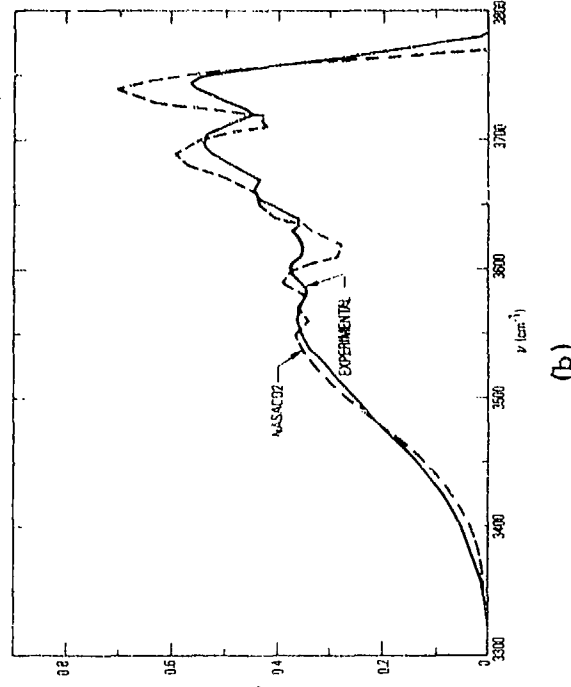
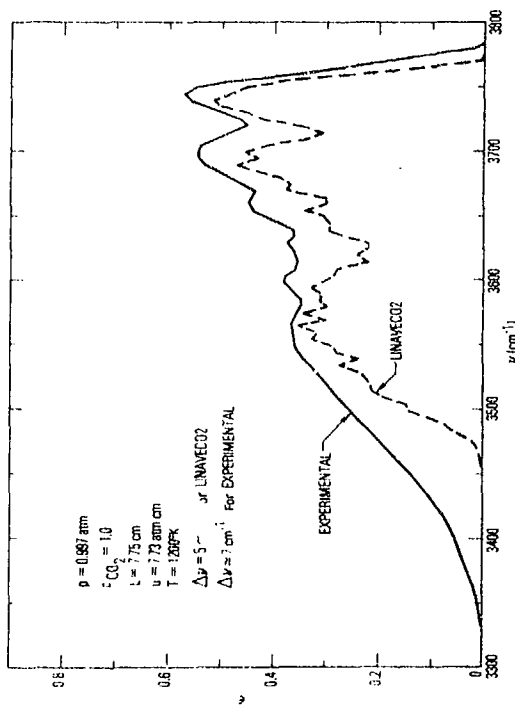


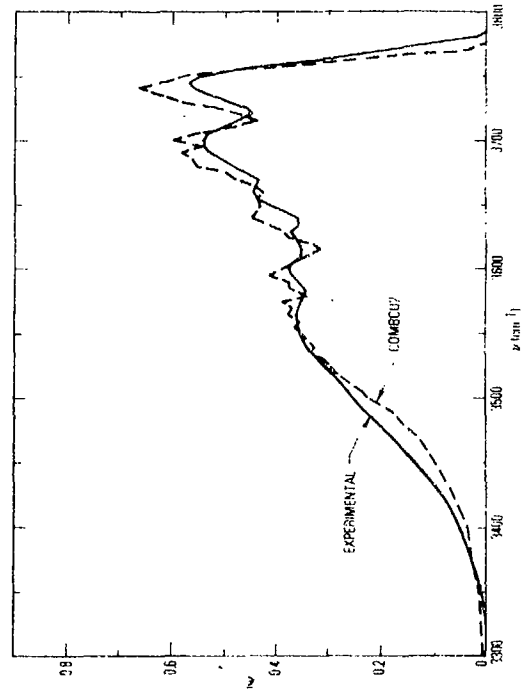
Fig. 2. Low-Temperature Transmission Spectra for  $\text{CO}_2$  in the Band Wing Region. The LINAVECO<sub>2</sub> and NASACO<sub>2</sub> curves show spectra computed with the indicated band model parameter set. The EXPERIMENTAL curve is derived from the tables of Ref. 9 for sample no. 1 and for  $\Delta\nu = 5 \text{ cm}^{-1}$ .



(a)



(b)



(c)

Fig. 3. High-Temperature Emission Spectra for  $\text{CO}_2$ . The LINAVECO<sub>2</sub> (a), NASA CO<sub>2</sub> (b), and COMBCO<sub>2</sub> (c) curves show spectra computed with the indicated band model parameter set. The EXPERIMENTAL curve is taken from Ref. 10.

parameters, on the other hand, provide results that are in excellent agreement with the experimental spectrum for the whole spectral region below  $\nu \approx 3600$   $\text{cm}^{-1}$  and that are in adequate agreement for the rest of the band.

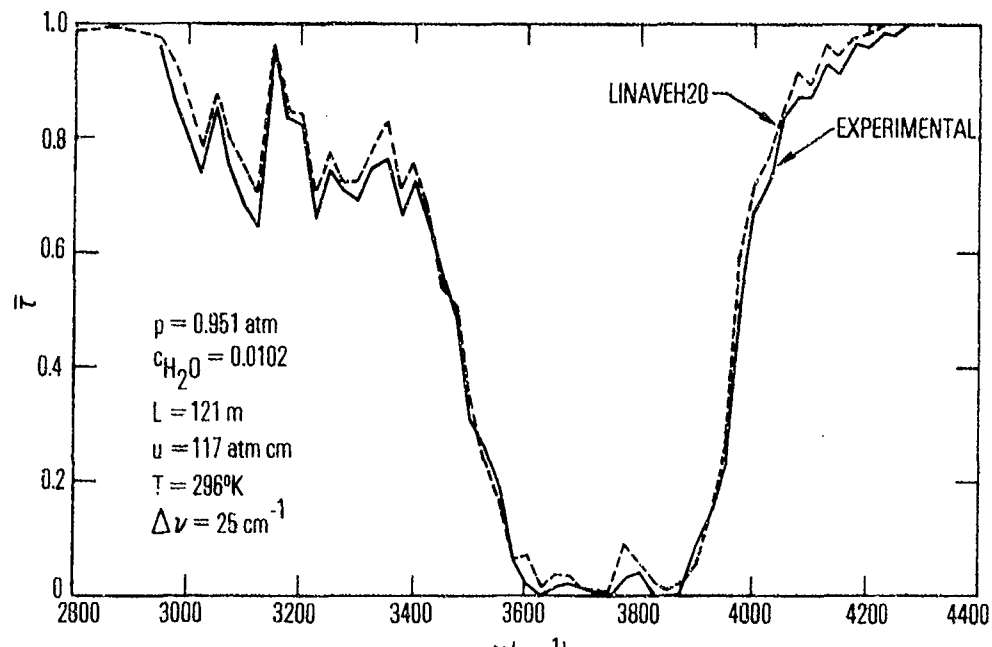
### 3. $\text{H}_2\text{O}$ At 296°K

High-resolution spectra and tables of integrated absorptance similar to those of  $\text{CO}_2$  are given for  $\text{H}_2\text{O}$  by Burch et al.<sup>11</sup> The solid curve of Fig. 4 is the transmittance spectrum for sample no. 39 with  $p = 0.951$  atm,  $c = 0.0102$  (with  $\text{N}_2$  as the remaining gas), and  $L = 121$  m. The optical thickness is  $u = 117$  atm cm and  $\Delta\nu = 25$   $\text{cm}^{-1}$ . Figure 4(a) shows the comparison of the experimental spectrum with the spectrum computed with the LINAVEH $\text{H}_2\text{O}$  parameters. The agreement between the two spectra is very good over the whole region from 2950 to 4300  $\text{cm}^{-1}$ . Figure 4(b) displays the comparison with the result obtained using the NASAH $\text{H}_2\text{O}$  parameters. As for  $\text{CO}_2$ , only a general qualitative agreement exists between the two curves; the quantitative agreement is decidedly poor.

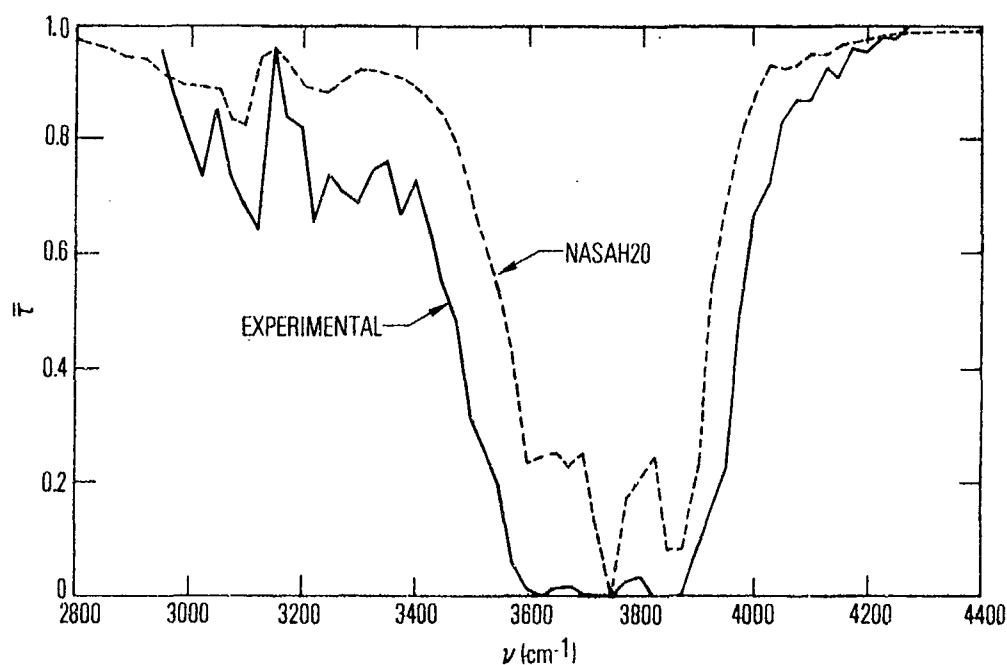
A comparison in the band center region from 3400 to 4200  $\text{cm}^{-1}$  for a less absorbing sample is given in Fig. 5. The experimental conditions (sample no. 38) are:  $p = 0.176$  atm,  $c = 0.031$ ,  $L = 4.16$  m, and  $u = 2.27$  atm cm. Again, the LINAVEH $\text{H}_2\text{O}$  parameters yield excellent agreement with experiment and the NASAH $\text{H}_2\text{O}$  parameters, poor agreement.

A more strongly absorbing sample (sample no. 40) with  $p = 0.20$  atm,  $c = 0.101$ ,  $L = 933$  m, and  $u = 1875$  atm cm was used to show comparison in the wing region from 2800 to 3500  $\text{cm}^{-1}$ . The results are given in Fig. 6 and again display the adequacy of the LINAVEH $\text{H}_2\text{O}$  parameters and the inadequacy of the NASAH $\text{H}_2\text{O}$  parameters at yielding accurate low-temperature  $\text{H}_2\text{O}$  absorption spectra.

<sup>11</sup>D. E. Burch, D. A. Gryvnak, and R. R. Patty, Absorption by  $\text{H}_2\text{O}$  Between 2800 and 4500  $\text{cm}^{-1}$  (2.7 Micron Region), U-3202, Aeronutronic Div., Philco-Ford Corp., Newport Beach, Calif. (30 September 1965).



(a)



(b)

Fig. 4. Low-Temperature Transmission Spectra for  $\text{H}_2\text{O}$ . The LINAVEH2O (a) and NASAH2O (b) curves show spectra computed with the indicated band model parameter set. The EXPERIMENTAL curve is derived from the tables of Ref. 11 for sample no. 39 and for  $\Delta\nu = 25 \text{ cm}^{-1}$ .

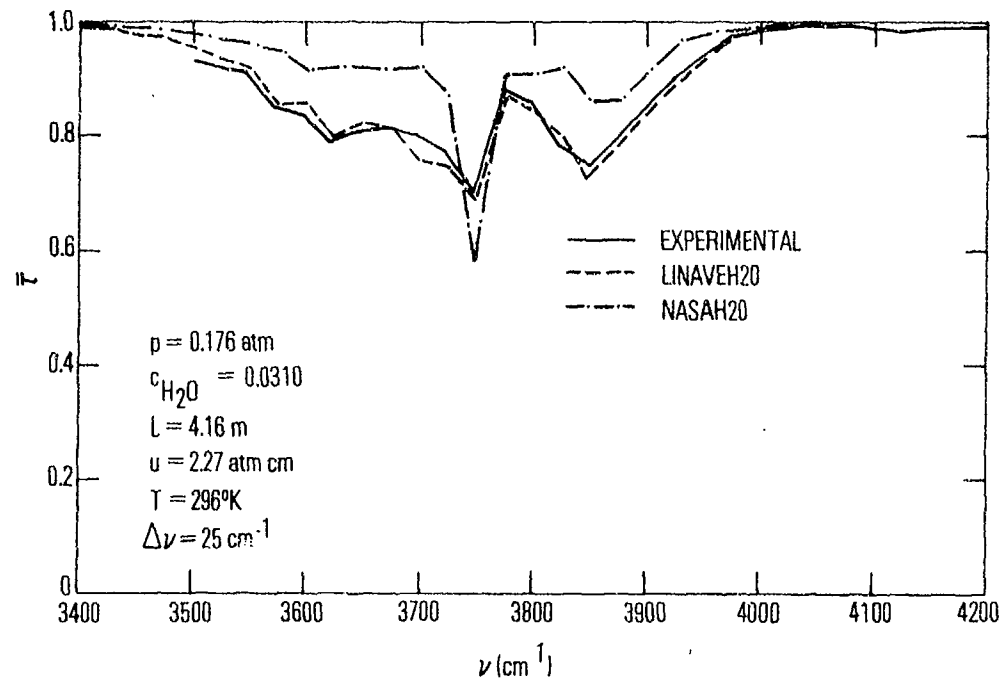


Fig. 5. Low-Temperature Transmission Spectra for  $\text{H}_2\text{O}$  in the Band Center Region. The LINAVEH $\text{H}_2\text{O}$  and NASAH $\text{H}_2\text{O}$  curves show spectra computed with the indicated band model parameter set. The EXPERIMENTAL curve is derived from the tables of Ref. 11 for sample no. 38 and for  $\Delta\nu = 25 \text{ cm}^{-1}$ .

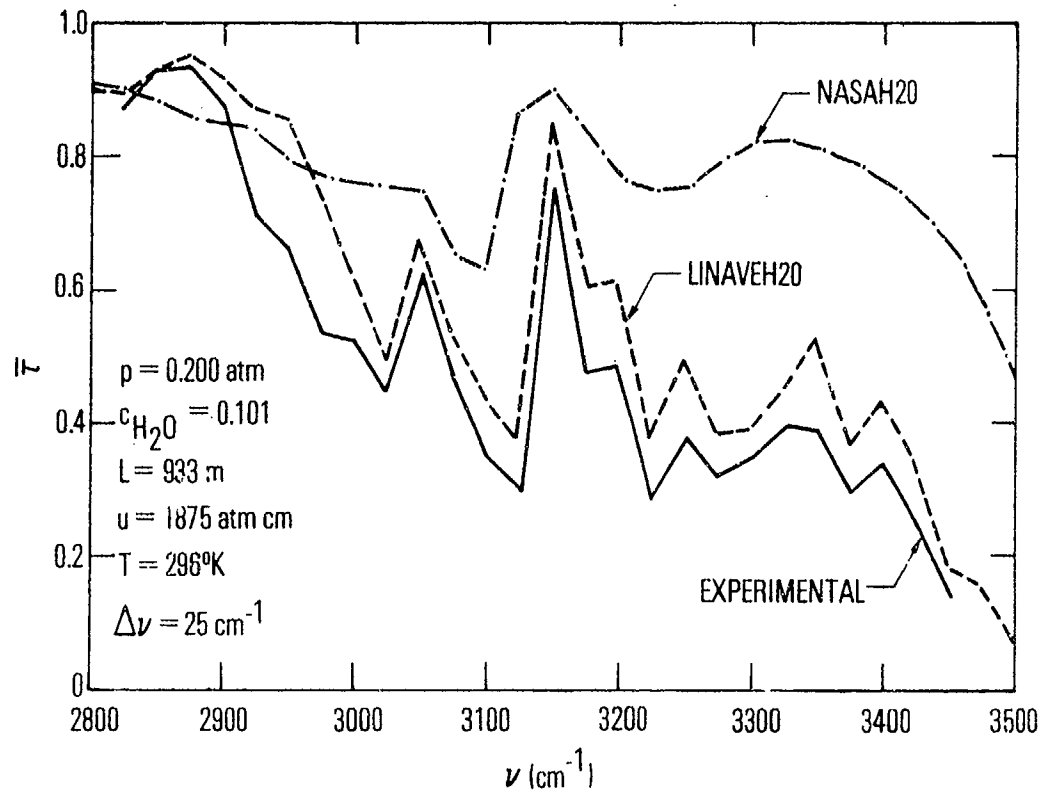


Fig. 6. Low-Temperature Transmission Spectra for  $\text{H}_2\text{O}$  in the Band Wing Region. The LINAVEH $\text{H}_2\text{O}$  and NASAH $\text{H}_2\text{O}$  curves show spectra computed with the indicated band model parameter set. The EXPERIMENTAL curve is derived from the tables of Ref. 11 for sample no. 40 and for  $\Delta\nu = 25 \text{ cm}^{-1}$ .

#### 4. $\text{H}_2\text{O}$ AT $1040^\circ\text{K}$

A medium resolution emissivity spectrum for pure  $\text{H}_2\text{O}$  given by Simmons et al.<sup>12</sup> was used for this comparison. The experimental conditions are:  $p = 0.937 \text{ atm}$ ,  $c = 1.00$ ,  $L = 60 \text{ cm}$ ,  $T = 1040^\circ\text{K}$ , and  $u = 56.2 \text{ atm cm}$ . The experimental spectrum and the results using the LINAVEH<sub>2</sub>O parameters are shown in Fig. 7(a) while the results using the NASAH<sub>2</sub>O parameters are shown in Fig. 7(b). In the band center region between  $3400$  and  $4050 \text{ cm}^{-1}$ , either set approximately reproduces the band contour of the experimental result, with the LINAVEH<sub>2</sub>O parameters possibly giving a slightly better fit. In the wing regions above  $4050 \text{ cm}^{-1}$  and below  $3400 \text{ cm}^{-1}$ , the LINAVEH<sub>2</sub>O parameters significantly underestimate the emissivity. The NASAH<sub>2</sub>O parameters, on the other hand, provide results that are in excellent agreement with the experimental wing contours. There is a general underestimation of the emissivity by the NASAH<sub>2</sub>O parameters between  $3400$  and  $3700 \text{ cm}^{-1}$ . It should be remembered, however, that even at this temperature, these parameters are not experimentally measured but are extrapolated from higher temperature measurements. An example of the good fit between measured and computed values at  $2500^\circ\text{K}$  is given in Ref. 3.

These comparisons confirm the initial suspicions that the LINAVE parameters should be adequate for low-temperature applications but deficient at high temperatures whereas the converse is generally true for the NASA parameters. To summarize the comparison results:

1. The LINAVE parameters are adequate for both  $\text{CO}_2$  and  $\text{H}_2\text{O}$  throughout the  $2.7\text{-}\mu\text{m}$  bands of these species for  $T \approx 300^\circ\text{K}$ .
2. The LINAVE parameters are adequate near the  $2.7\text{-}\mu\text{m}$  band centers for temperatures at least as high as  $T \approx 1000^\circ\text{K}$  but are inadequate in the band wings for this and higher temperatures. This holds for both  $\text{H}_2\text{O}$  and  $\text{CO}_2$ .

<sup>12</sup>F. S. Simmons, C. B. Arnold, and D. H. Smith, Studies of Infrared Radiative Transfer in Hot Gases, I: Spectral Absorptance Measurements in the  $2.7\mu \text{ H}_2\text{O Bands}$ , Rep. No. 4613-91-T, Willow Run Laboratory, Ann Arbor, Mich. (August 1965).

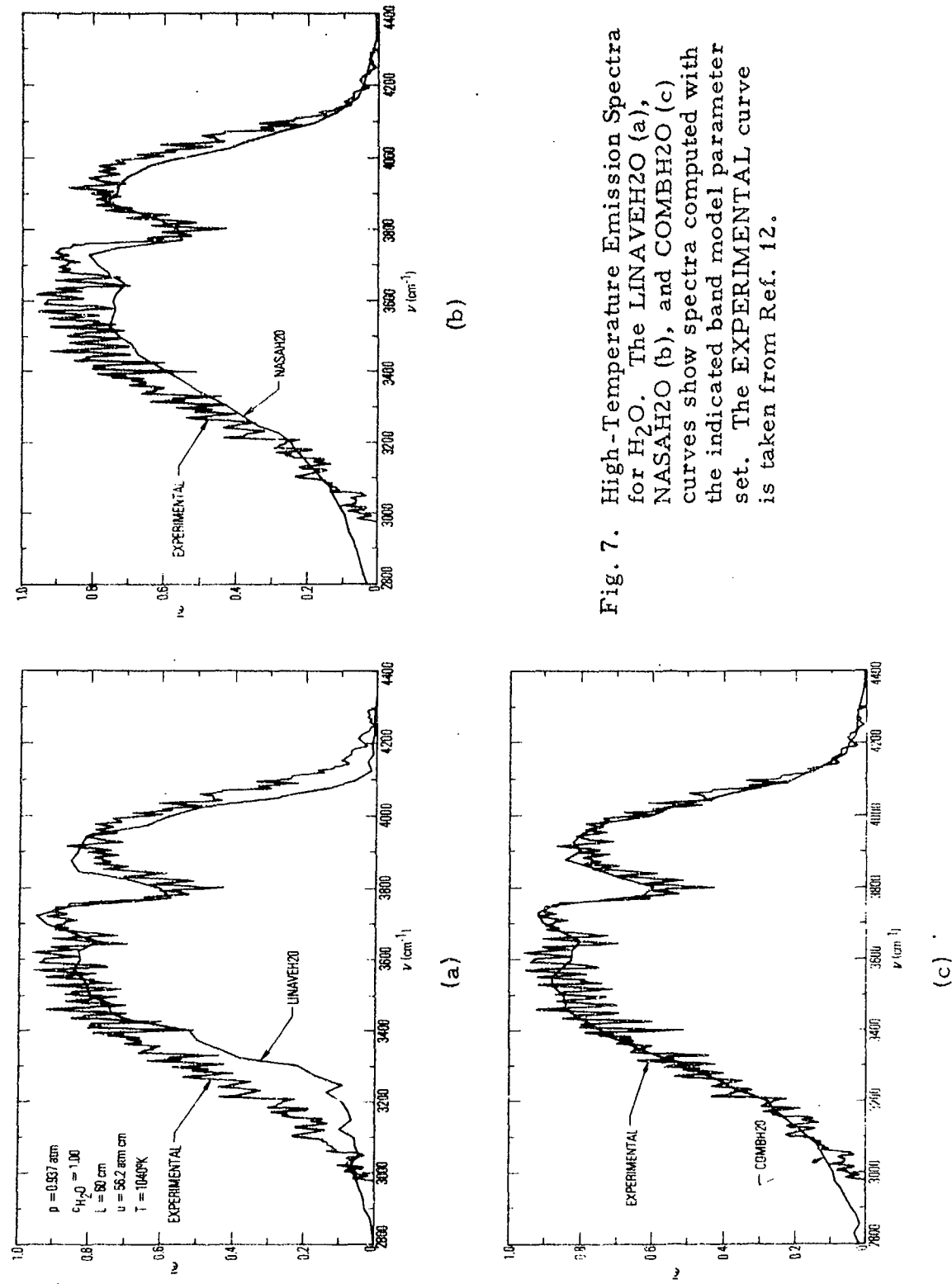


Fig. 7. High-Temperature Emission Spectra for  $H_2O$ . The LINAVEH2O (a), NASAH2O (b), and COMBH2O (c) curves show spectra computed with the indicated band model parameter set. The EXPERIMENTAL curve is taken from Ref. 12.

3. The NASA parameters are adequate for both CO<sub>2</sub> and H<sub>2</sub>O throughout the 2.7-μm bands of these species for temperatures above T ≈ 1000°K.
4. The NASA parameters are inadequate for both H<sub>2</sub>O and CO<sub>2</sub> anywhere in the 2.7-μm spectral region for T ≈ 300°K.

### III. COMBINED PARAMETER SETS

#### A. GENERAL PROCEDURE

Parameter sets for both  $\text{CO}_2$  and  $\text{H}_2\text{O}$  that are consistent for the whole temperature range from 100 to  $3000^{\circ}\text{K}$  were generated by combining the low-temperature variation of the LINAVE parameters with the high-temperature variation of the NASA parameters. This combination was performed at each spectral position by making semilogarithmic plots of the parameters from each set as functions of temperature, and connecting some "low" temperature point on the LINAVE curve with some "high" temperature point on the NASA curve. The designations "low" and "high" temperature are relative terms only, since the connection at some spectral positions was best done by connecting, for example, the  $1000^{\circ}\text{K}$  value for the LINAVE parameter with the  $1500^{\circ}\text{K}$  value for the NASA parameter or, in other cases, the  $250^{\circ}\text{K}$  value of the LINAVE parameter with the  $300^{\circ}\text{K}$  value for the NASA parameter. Examples of the method are given in Figs. 8 through 11 for several spectral intervals for both  $\text{CO}_2$  and  $\text{H}_2\text{O}$ .

This procedure is admittedly subjective, although several rules and guidelines were followed for making the transition from one curve to the other:

1. The transition from one curve to the other should make the overall variation as smooth as possible.
2. The LINAVE parameters for  $T \leq 300^{\circ}\text{K}$  should remain reasonably unchanged.
3. The NASA parameters for  $T \geq 2000^{\circ}\text{K}$  should remain reasonably unchanged.
4. No redefinition of parameter values in either set is made. The temperature variation of the combined set consists of established values from one set or the other, or values interpolated from the transition line.
5. The match-up for each spectral interval should be consistent with the match-up made for adjacent spectral intervals.
6. The match-up for  $\delta_e$  should reflect a monotonic increase of the density ( $1/\delta_e$ ) with temperature.

Even with these guidelines, several ways of connecting the sets were sometimes possible. An iterative procedure was used in these cases. A first-guess match-up was made and spectra generated for the homogeneous path conditions described in the previous section. A comparison of these spectra with the experimental curves and inspection of the parameter plots were made to see if another transition line would give a better result. If it could, the change was made and tested by generating new spectra for comparison.

#### B. H<sub>2</sub>O PARAMETER SET (COMBH2O)

Parameter plots for both  $\bar{k}$  and  $1/\delta_e$  were made for 81 spectral positions from 2500 to 4500 cm<sup>-1</sup> (equal steps of 25 cm<sup>-1</sup>). The four main types of variations for  $\bar{k}$  that occurred are shown in Fig. 8. The LINAVEH<sub>2</sub>O variation displayed in Fig. 8(a) ( $\nu = 2500 \text{ cm}^{-1}$ ) is typical for all of the spectral intervals in the band wing region. The absorption coefficient increases with temperature up to  $\sim 1000^\circ\text{K}$  but thereafter levels off or falls slightly. The increasing discrepancy between the LINAVEH<sub>2</sub>O and the NASAH<sub>2</sub>O curves reflects the lack of hot band lines in the AFCRL atlas for the wing region.

Figures 8(a) ( $\nu = 2500 \text{ cm}^{-1}$ ) and 8(d) ( $\nu = 4075 \text{ cm}^{-1}$ ) show variations in which several reasonable transition lines could be drawn. In the latter ( $\nu = 4075 \text{ cm}^{-1}$ ), the line from  $150^\circ\text{K}$  on the LINAVEH<sub>2</sub>O curve to  $300^\circ\text{K}$  on the NASAH<sub>2</sub>O curve was the first guess based on the "smoothness" criterion. Better overall agreement with the experimental spectra, however, was obtained using the transition line from  $300^\circ\text{K}$  on the LINAVEH<sub>2</sub>O curve to  $1000^\circ\text{K}$  on the NASAH<sub>2</sub>O curve. The variations at  $\nu = 3400$  and  $3700 \text{ cm}^{-1}$  [Figs. 8(b) and 8(c), respectively] are examples where little judgment was required to make the match-up. In general, throughout regions of strong absorption, the match-up procedure was relatively self-evident.

The variations of  $\delta_e$  for H<sub>2</sub>O with temperature were very consistent throughout the whole spectral region and were simple variations of the forms shown in Fig. 9. In all cases, the first-guess match-up was sufficient.

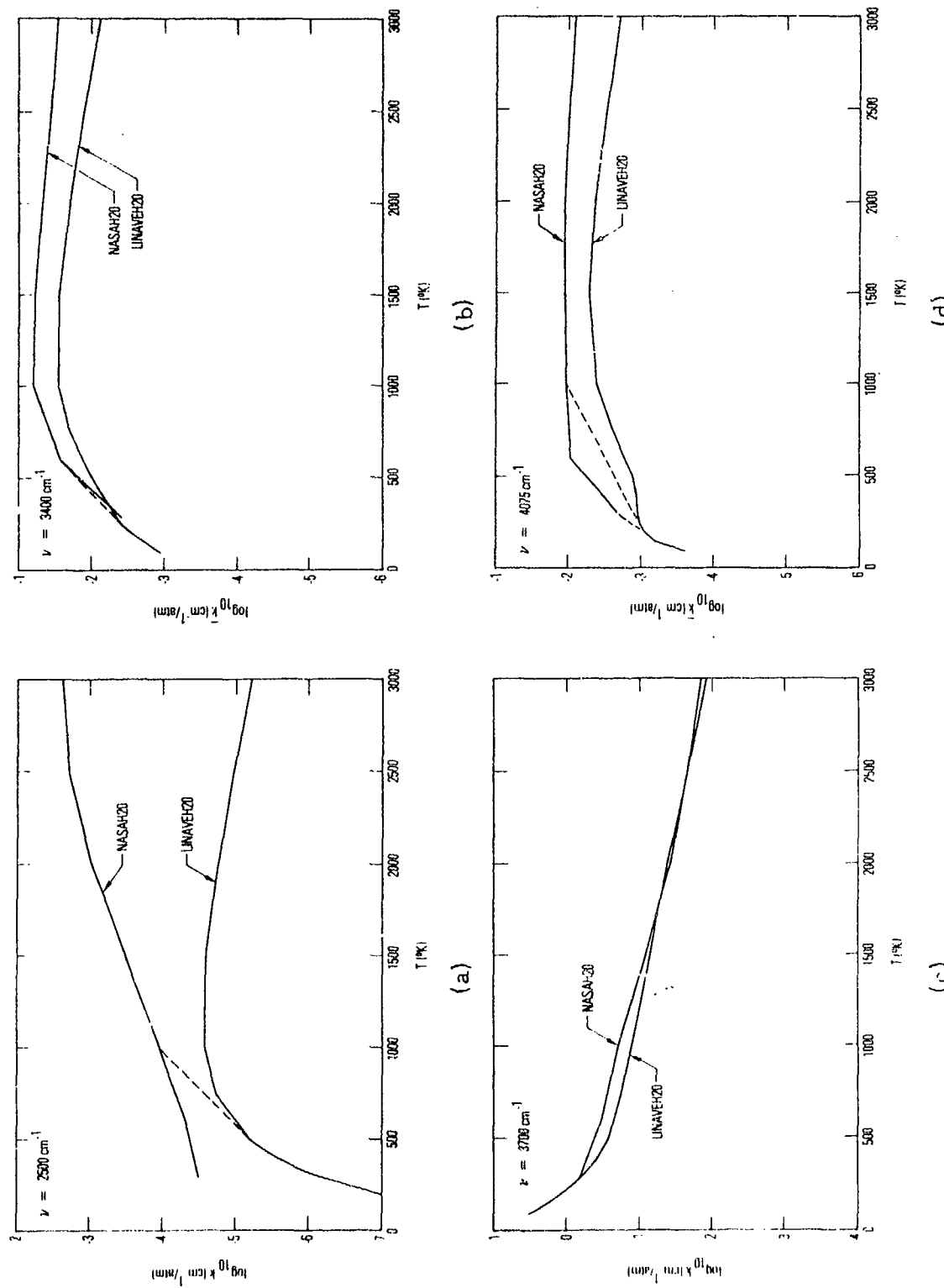
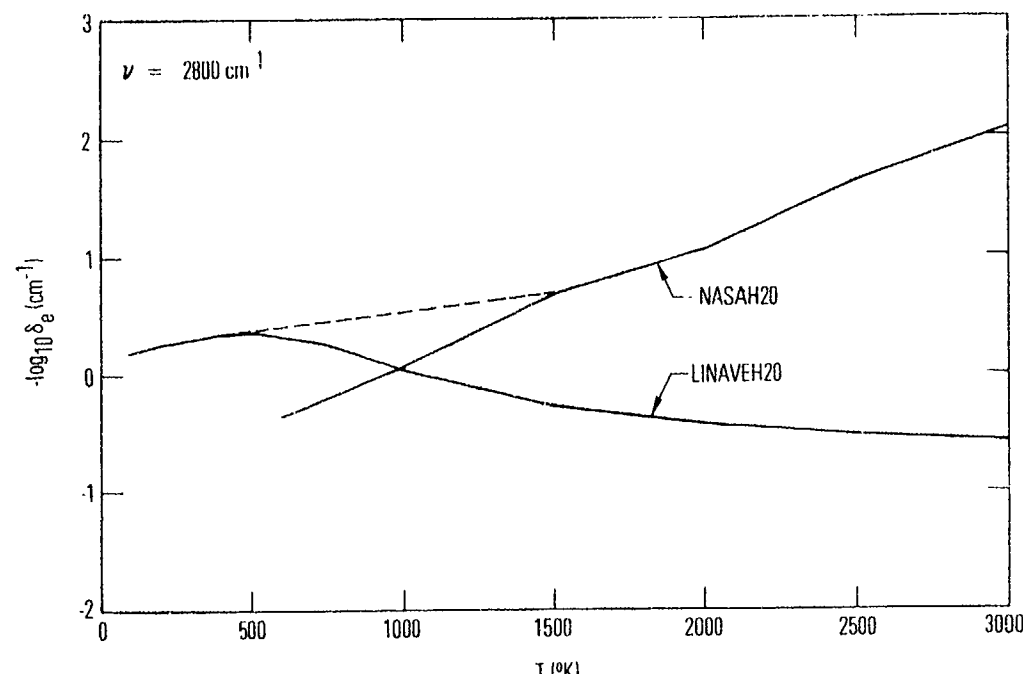
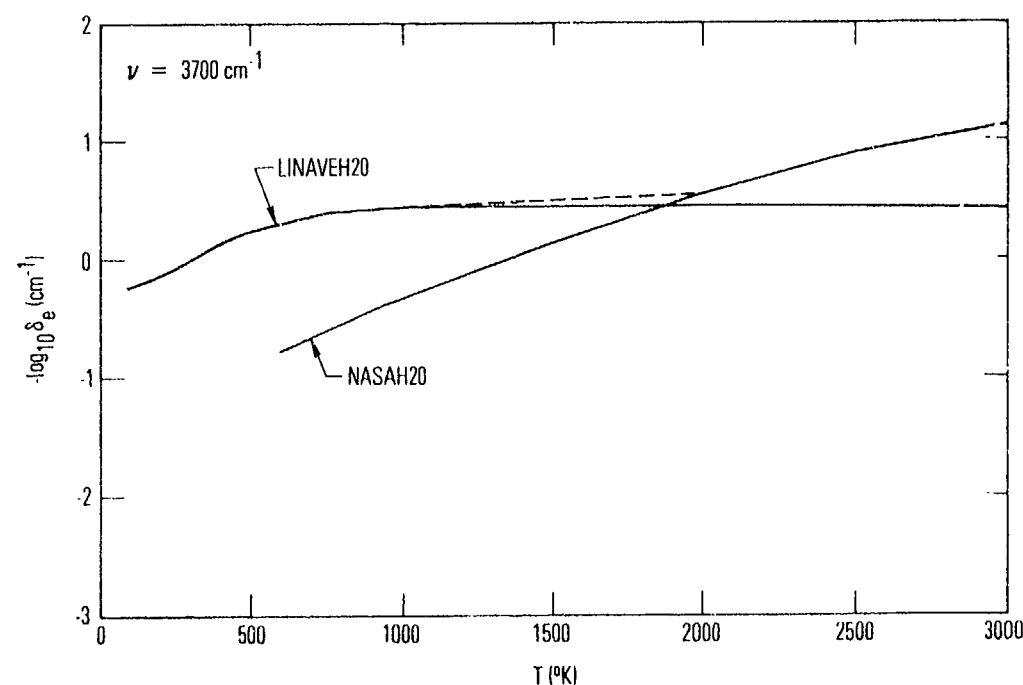


Fig. 8. Variation of  $\bar{K}(\text{H}_2\text{O})$  with Temperature for Selected Spectral Intervals. The LINAVEH<sub>2</sub>O and NASAH<sub>2</sub>O curves are the variations for the indicated band model parameter set; dashed curves show transitions from one curve to the other.



(a)



(b)

Fig. 9. Variation of  $1/\delta_e$  ( $\text{H}_2\text{O}$ ) with Temperature for Selected Spectral Intervals. The LINAVEH<sub>2</sub>O and NASAH<sub>2</sub>O curves are the variations for the indicated band model parameter set; dashed curves show transitions from one curve to the other.

A final parameter set was generated for  $\text{H}_2\text{O}$  for the spectral region  $\nu = 2500$  to  $4500 \text{ cm}^{-1}$  by steps of  $25 \text{ cm}^{-1}$  and reflects a spectral resolution of  $\Delta\nu = 25 \text{ cm}^{-1}$ . The ten temperature values  $T = 100, 200, 300, 500, 750, 1000, 1500, 2000, 2500$ , and  $3000^\circ\text{K}$  were chosen to represent the temperature variation. The mean line width parameter  $\bar{\gamma}_0$  from the LINAVEH $\text{H}_2\text{O}$  set was chosen to represent this parameter for the combined set. Spectra for the homogeneous path conditions of Sect. II were generated with the final parameter set to verify its validity. For all of the low-temperature cases, the spectra generated with the COMBH $\text{H}_2\text{O}$  parameters were indistinguishable (in plots) from those generated using the LINAVEH $\text{H}_2\text{O}$  parameters. The spectrum for the  $1040^\circ\text{K}$  path is shown in Fig. 7(c). The overall agreement with the experimental curve is better than was obtained with either the LINAVEH $\text{H}_2\text{O}$  or NASAH $\text{H}_2\text{O}$  parameters. A tabulation of the COMBH $\text{H}_2\text{O}$  parameter set is included in the Appendix.

#### C. $\text{CO}_2$ PARAMETER SET (COMBCO $\text{2}$ )

Parameter plots for  $\bar{k}$  and  $1/\delta_e$  were made for the 135 spectral positions from  $3100$  to  $3770 \text{ cm}^{-1}$  (equal steps of  $5 \text{ cm}^{-1}$ ). Examples of match-ups are illustrated in Fig. 10. In the band wing region, the variation of the LINAVE  $\bar{k}$  parameter is similar to that for  $\text{H}_2\text{O}$  in the wing region. That is, the value increases with temperature up to about  $500^\circ\text{K}$  and then decreases owing to the lack of data in the AFCRL compilation for hot band lines. The examples for  $\nu = 3525$  and  $3725 \text{ cm}^{-1}$  in Fig. 10 are cases where the match-up is easily made.

Examples of the match-up of the line spacing parameter  $\delta_e$  are shown in Fig. 11. In most cases, the selection of the transition line was reasonably self-evident.

After several match-up iterations, a final parameter set was generated for  $\text{CO}_2$  for the spectral region  $\nu = 3100$  to  $3770 \text{ cm}^{-1}$  by steps of  $5 \text{ cm}^{-1}$  and reflects a spectral resolution of  $\Delta\nu = 5 \text{ cm}^{-1}$ . The same ten temperatures as for  $\text{H}_2\text{O}$  were chosen to represent the temperature variation of the set.

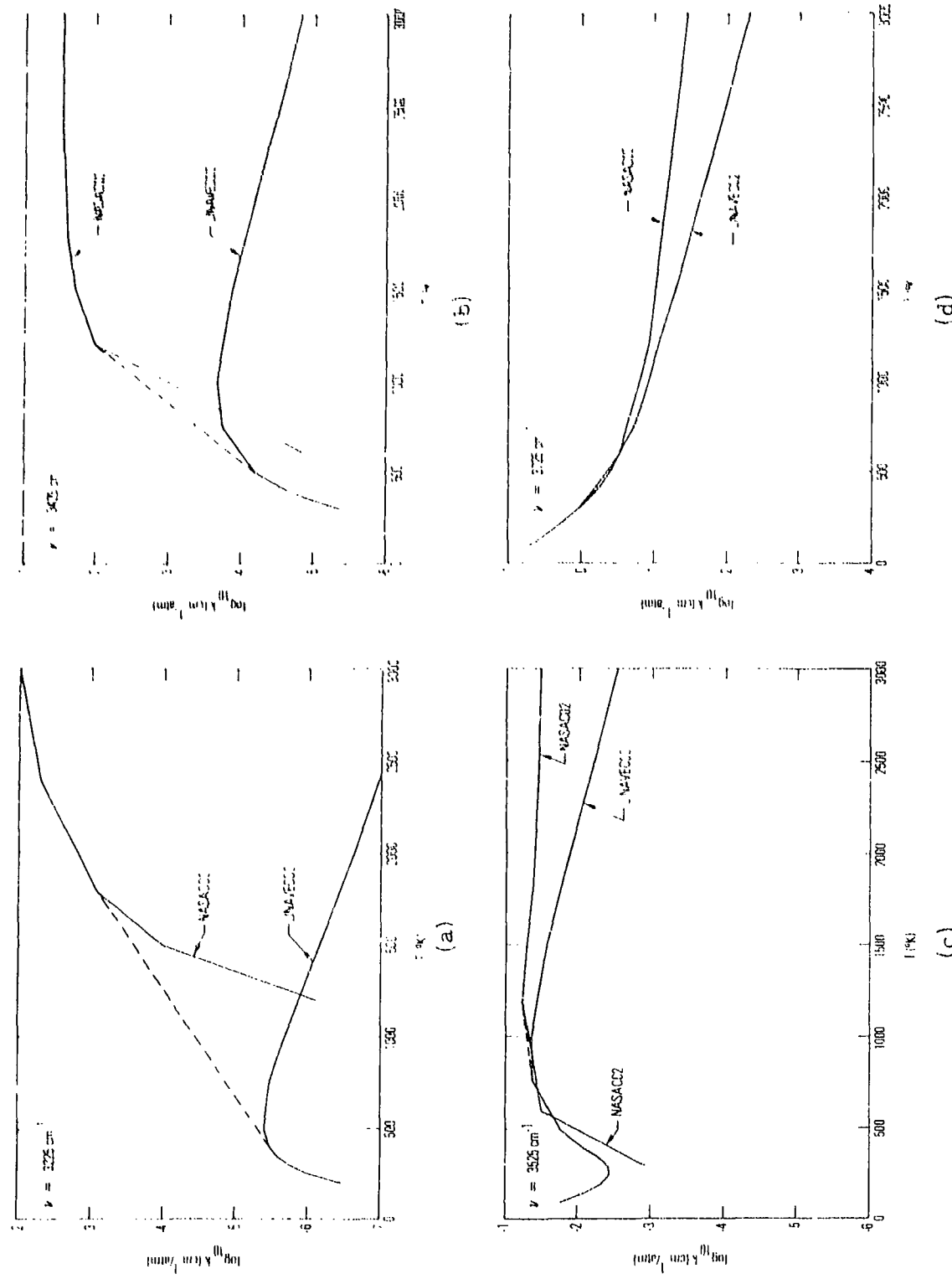
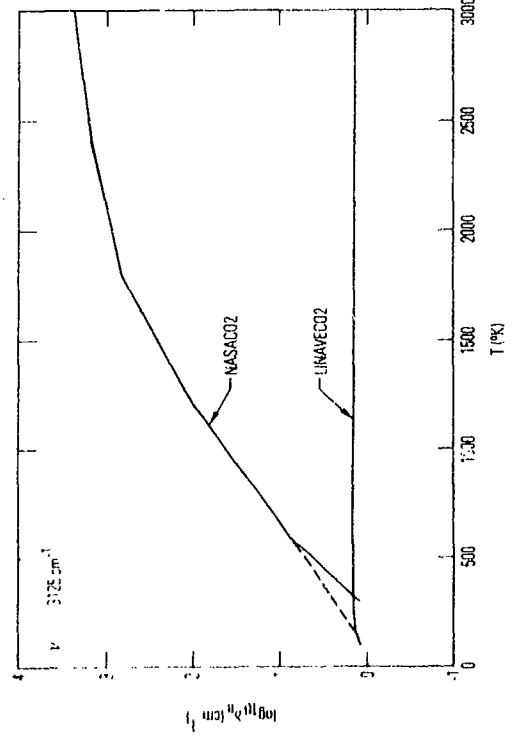
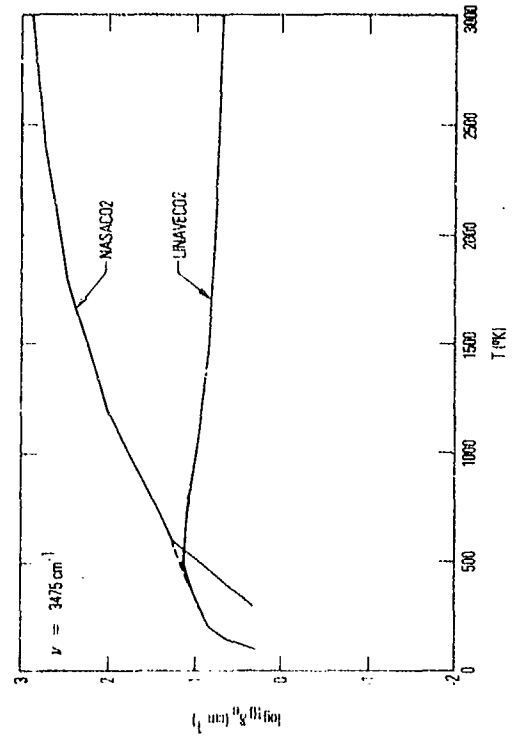


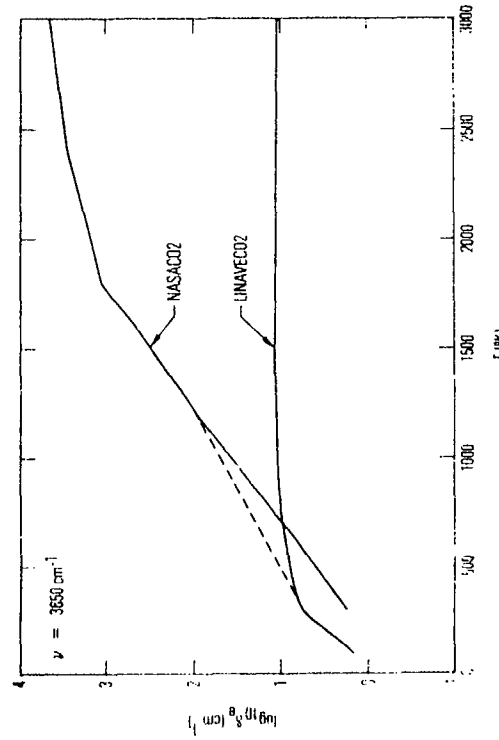
Fig. 10. Variation of  $\bar{k}(\text{CO}_2)$  with Temperature for Selected Spectral Intervals. The LINAVECO<sub>2</sub> and NASA CO<sub>2</sub> curves are the variations for the indicated band model parameter set; dashed curves show transitions from one curve to the other.



(a)



(b)



(c)

Fig. 11. Variation of  $1/\sigma_e(\text{CO}_2)$  with Temperature for Selected Spectral Intervals. The LINAVE CO<sub>2</sub> and NASA CO<sub>2</sub> curves are the variations for the indicated band model parameter set; dashed curves show transitions from one curve to the other.

The mean line width parameter  $\bar{\gamma}_0$  from the LINAVECO<sub>2</sub> set was chosen to represent this parameter in the final set. The  $\bar{k}$  and  $1/\delta_e$  parameters of the LINAVECO<sub>2</sub> set are zero for the 5-cm<sup>-1</sup> intervals centered on  $\nu = 3245$  and 3250 cm<sup>-1</sup> because no lines occur in these regions. The data from the NASACO<sub>2</sub> set for the whole temperature range were used for these intervals.

Spectra for the homogeneous path conditions of Sect. II were computed with the final parameter set to verify its validity. For the low-temperature cases, the results were indistinguishable from the LINAVECO<sub>2</sub> curves of Figs. 1 and 2 except in the 3625- and 3725-cm<sup>-1</sup> valleys, where a slight improvement in agreement with the experimental curve was noted. The spectrum for the 1200°K case is shown in Fig. 3(c). The overall agreement with the experimental curve is better than was obtained with either the LINAVECO<sub>2</sub> or NASACO<sub>2</sub> parameters. A tabulation of the COMBCO<sub>2</sub> parameters is included in the Appendix.

#### IV. ATMOSPHERIC TRANSMITTANCE CALCULATION

In Ref. 1, radiative transfer calculations for two atmospheric paths and a hypothetical hot H<sub>2</sub>O/CO<sub>2</sub> plume at 20-km altitude were made with either the LINA VE or NASA parameters. The results for the slant path (20 km to space at a 75-deg zenith angle) have been recomputed for the LINA VE and NASA parameters and are compared here with the results obtained using the COMB parameters. The source path represents a single line of sight through the diameter position of a homogeneous, isothermal, circular cylindrical plume at an aspect angle of 90 deg. The source path length is 7.73 m, the temperature is 1249°K, the mole fraction of H<sub>2</sub>O is 0.2533, and the mole fraction of CO<sub>2</sub> is 0.03714. A tropical model atmosphere was used.<sup>13</sup> The calculations were performed for the Lorentz line shape, with an exponential-tailed inverse line strength distribution, and used the Lindquist-Simmons approximation.

The band model parameters for CO<sub>2</sub> were reduced in resolution from 5 to 25 cm<sup>-1</sup> in order to be compatible with the resolution of the H<sub>2</sub>O parameters. The band model parameters for the 5-cm<sup>-1</sup>-wide interval centered on  $\nu_i$  and the parameters for the two lower and two higher adjacent intervals were averaged to give the parameters for the 25-cm<sup>-1</sup>-wide interval centered on  $\nu_i$  according to

$$\bar{k} = \frac{1}{5} \sum_{j=i-2}^{i+2} \bar{k}(j)$$

<sup>13</sup>R. A. McClatchey, R. W. Fenn, J. E. A. Selby, F. E. Volz, and J. S. Garing, Optical Properties of the Atmosphere (Revised), AFCLR-71-0279, Air Force Cambridge Research Laboratories, Mass. (10 May 1971).

$$\bar{\gamma}_0 = \frac{1}{5} \sum_{j=i-2}^{i+2} \bar{\gamma}_0(j)$$

and

$$\frac{1}{\delta_e} = \frac{1}{k \bar{\gamma}_0} \left[ \frac{1}{5} \sum_{j=i-2}^{i+2} \sqrt{\frac{\bar{k}(j) \bar{\gamma}_0(j)}{\delta_e(j)}} \right]^2$$

The results obtained with the three parameter sets for the radiance at the boundary of the source and after transmission along the absorbing atmospheric path are shown in Fig. 12. The transmittance  $\bar{\tau}$ , obtained without account of line correlation, is illustrated in Fig. 13. Similarly, the effective transmittance of the atmosphere  $\bar{\tau}_e$ , obtained by taking account of line correlation between the source emission spectrum and the atmospheric absorption spectrum, is given in Fig. 14. Detailed discussions of the source radiance and atmospheric transmittance  $\bar{\tau}$  spectra are not required since these would parallel those already given in Sect. II of this report. The only new result displayed by these spectra is the effective transmittance  $\bar{\tau}_e$  (Fig. 14). Although  $\bar{\tau}_e$  is a source-dependent quantity and, therefore, depends on the band model parameters used to describe the source emission, there is a great similarity between the  $\bar{\tau}_e$  spectra computed using the LINAVE and COMB parameters. A comparison between the NASA and COMB results, on the other hand, reveals a significant dissimilarity. These results would indicate that an accurate description of the atmosphere (that is, an accurate knowledge of band model parameters for low temperatures) is more important than an accurate description of the hot gas source in determining  $\bar{\tau}_e$ .

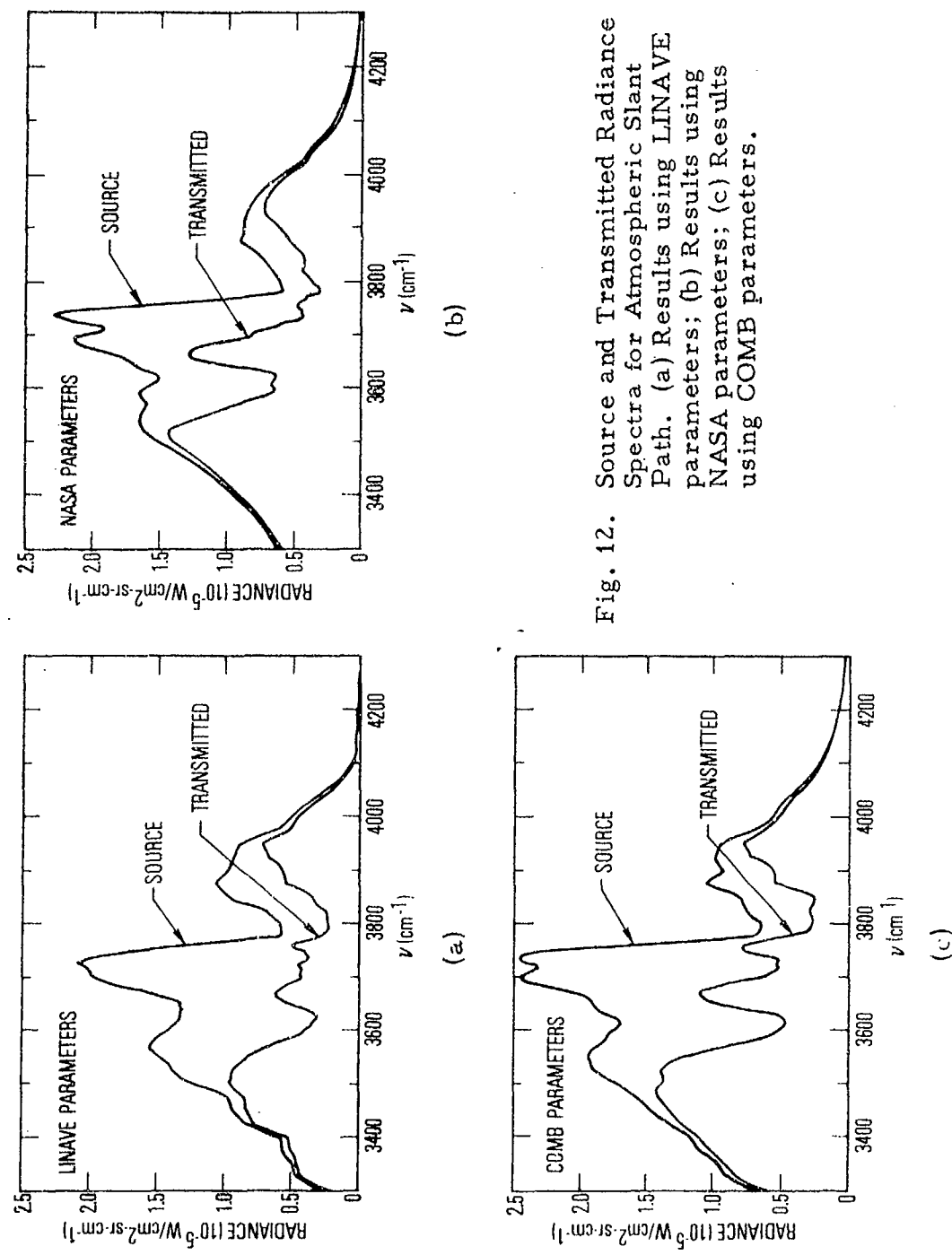


Fig. 12. Source and Transmitted Radiance Spectra for Atmospheric Slant Path. (a) Results using LINAVE parameters; (b) Results using NASA parameters; (c) Results using COMB parameters.

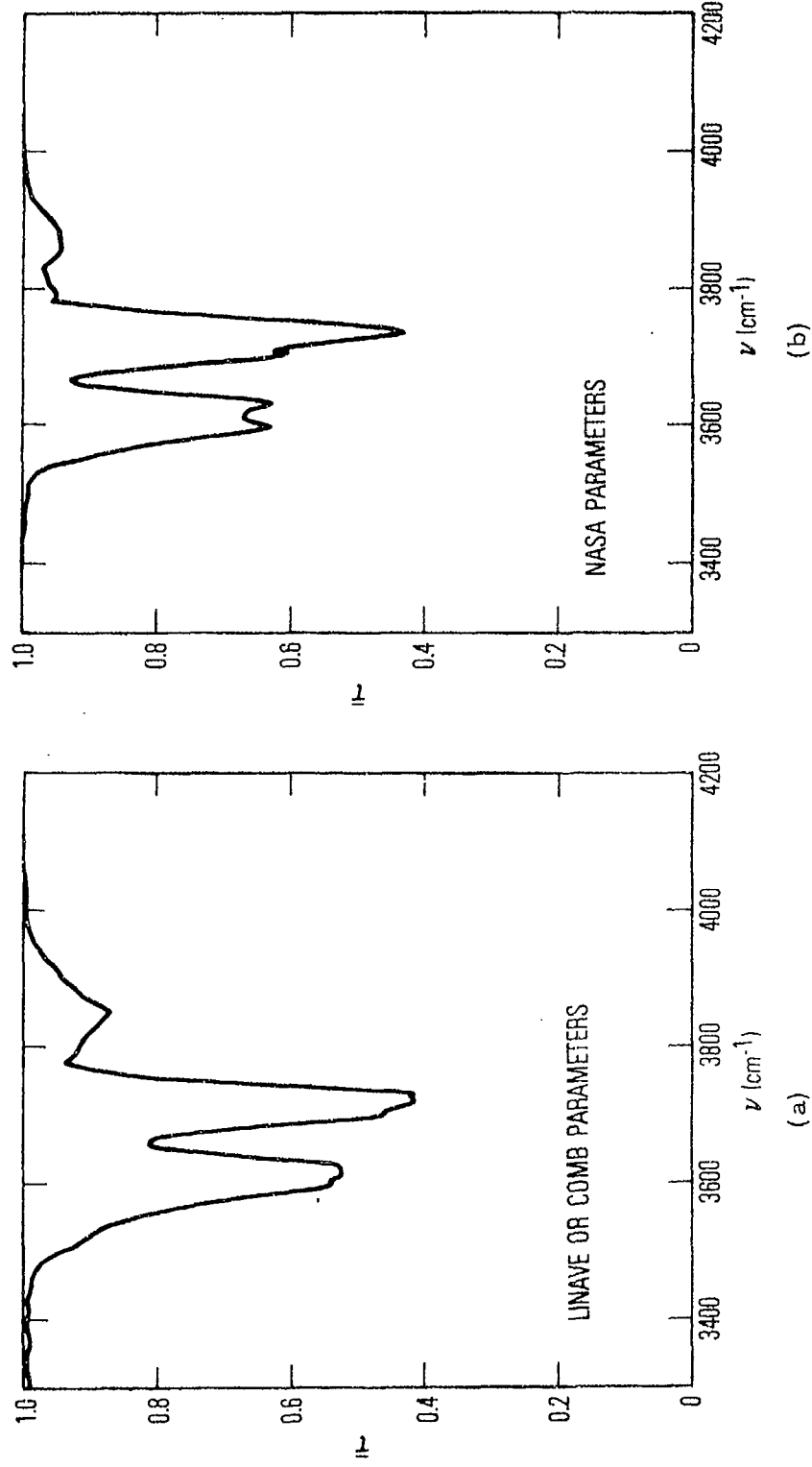


Fig. 13. Transmittance Spectra for Atmospheric Slant Path. (a) Results using LINAVE or COMB parameters; (b) Results using NASA parameters.

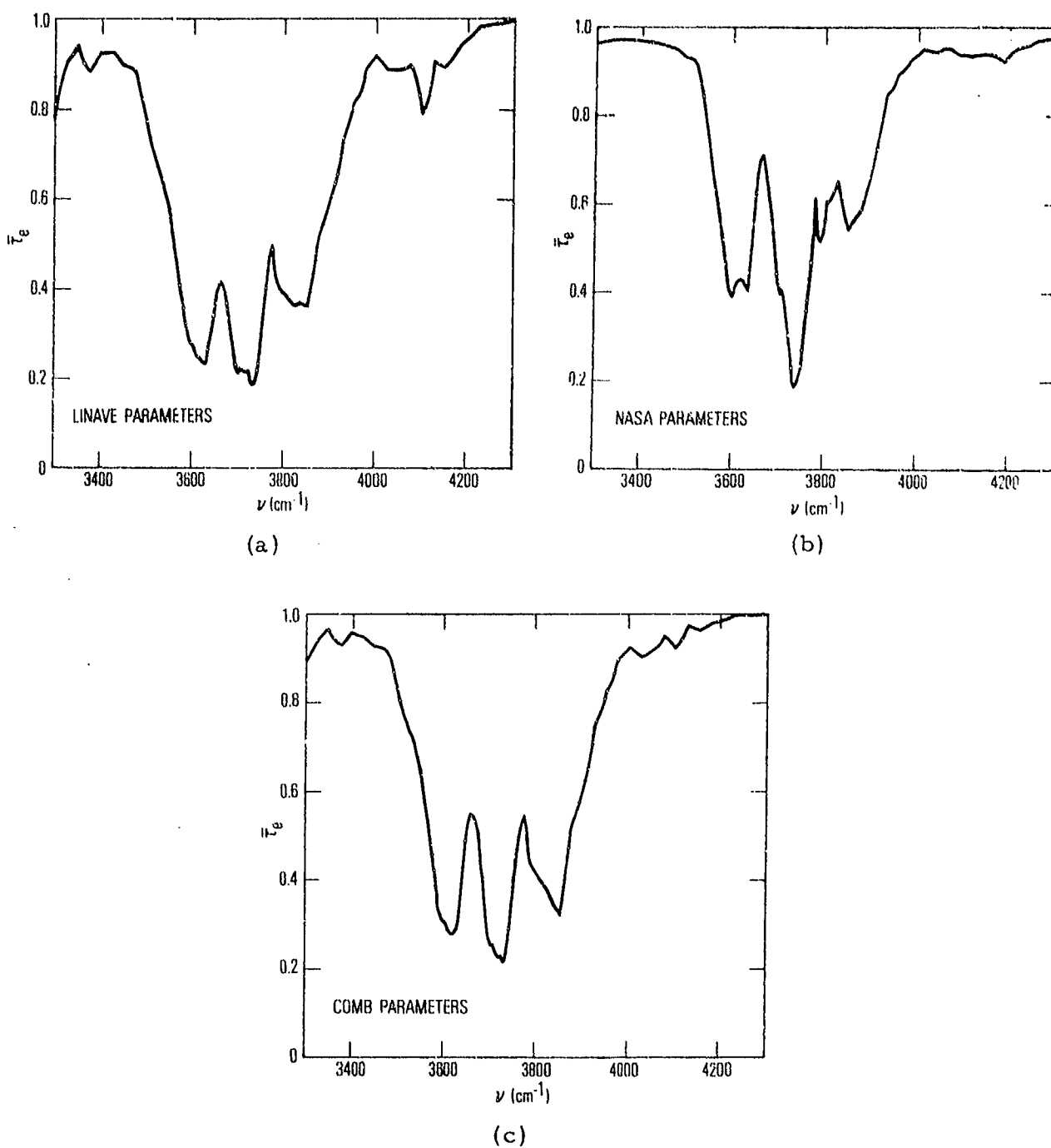


Fig. 14. Effective Transmittance Spectra for Atmospheric Slant Path.  
 (a) Results using LINAVE parameters; (b) Results using NASA parameters;  
 (c) Results using COMB parameters.

## APPENDIX

### COMBH2O AND COMBCO2 PARAMETER SET LISTINGS

Tabulations of the COMBH2O and COMBCO2 parameters are given in Tables A1 and A2, respectively. A description of these listings follows. IDNAME is simply an identification name for the parameter set. RESOLUTION is the value of  $\Delta\nu$  appropriate for the set. ALPHA (1) through ALPHA (5) are the ratios of the efficiency of pressure broadening by the indicated mechanisms to that of nonresonant self-broadening. ALPHA (6) is the atomic mass of the absorbing species. The WAVENUMBER array lists the center value of all the  $\Delta\nu$  intervals included in the set. NW is the number of such intervals. The TEMPERATURE array similarly lists the temperatures for which the data are tabulated. NT is the number of such temperatures. The ABSORPTION COEFFICIENT array is  $\bar{k}$ . The first column of this array is the interval center wave number, and the rows are the values at the temperatures of the TEMPERATURE array. The EFFECTIVE LINE DENSITY array is the parameter  $1/\delta_e$  and is presented in the same format as  $\bar{k}$ . The MEAN LINE WIDTH array is the parameter  $\bar{\gamma}_0$  for nonresonant self-broadening at STP. The values correspond to the wave numbers listed in the WAVENUMBER array.

Table A1. Listing of COMBH2O Band Model Parameter Set

Table A1. Listing of COMBH2O Band Model Parameter Set (Cont'd)

Table A1. Listing of COMBH2O Band Model Parameter Set (Cont'd)

EFFECTIVE LINE DENSITY(?)		ARRAY(LINES/C4-1)
4.376	*.00	5.0 329F-03 4.0 560E-07 2.0 659E-05 3.0 123E-06 4.0 305E-05 2.0 931E-05
4.462	*.00	3.0 962E-08 2.0 626E-07 1.0 149E-06 5.0 122E-06 5.0 245E-06 2.0 874E-05 3.0 224E-05 4.0 312E-04
4.450	*.00	9.0 209E-08 5.0 557E-07 1.0 635E-06 6.0 740E-06 7.0 390E-05 2.0 611E-05 3.0 433E-05 2.0 215E-05
4.475	*.00	9.0 999F-07 5.0 401F-07 3.0 412E-06 2.0 744F-06 2.0 101F-06 3.0 228E-05 8.0 605E-05
4.500	*.00	2.0 515F-07 7.0 101F-06 2.0 101F-06 3.0 228E-05 8.0 605E-05
4.500	*.00	1.0 537E+01 1.0 991F+00 2.0 190F+01 2.0 649E+03 3.0 360E+03 3.0 148E+03
2.550	*.00	1.0 115F+02 1.0 677E+02 2.0 811E+02 2.0 355E+02 2.0 365E+02 2.0 365E+02
2.675	*.00	1.0 119E+00 1.0 139E+00 2.0 156E+00 2.0 158E+00 2.0 158E+00 2.0 158E+00
2.625	*.00	1.0 154E+00 1.0 162E+00 2.0 164E+00 2.0 164E+00 2.0 164E+00 2.0 164E+00
2.650	*.00	1.0 187E+00 1.0 195E+00 2.0 197E+00 2.0 197E+00 2.0 197E+00 2.0 197E+00
2.675	*.00	6.0 377E+00 1.0 439E+00 2.0 215E+00 2.0 215E+00 2.0 215E+00 2.0 215E+00
2.770	*.00	1.0 340E+00 1.0 342E+00 2.0 326E+00 2.0 326E+00 2.0 326E+00 2.0 326E+00
2.772	*.00	1.0 350E+00 1.0 352E+00 2.0 326E+00 2.0 326E+00 2.0 326E+00 2.0 326E+00
2.775	*.00	1.0 377E+00 1.0 379E+00 2.0 326E+00 2.0 326E+00 2.0 326E+00 2.0 326E+00
2.775	*.00	1.0 377E+00 1.0 379E+00 2.0 326E+00 2.0 326E+00 2.0 326E+00 2.0 326E+00
2.800	*.00	1.0 377E+00 1.0 379E+00 2.0 326E+00 2.0 326E+00 2.0 326E+00 2.0 326E+00
2.825	*.00	1.0 411E+00 1.0 413E+00 2.0 326E+00 2.0 326E+00 2.0 326E+00 2.0 326E+00
2.825	*.00	1.0 411E+00 1.0 413E+00 2.0 326E+00 2.0 326E+00 2.0 326E+00 2.0 326E+00
2.875	*.00	1.0 576E+00 2.0 119E+00 2.0 123E+00 2.0 123E+00 2.0 123E+00 2.0 123E+00
2.900	*.00	1.0 576E+00 2.0 119E+00 2.0 123E+00 2.0 123E+00 2.0 123E+00 2.0 123E+00
2.925	*.00	1.0 576E+00 2.0 119E+00 2.0 123E+00 2.0 123E+00 2.0 123E+00 2.0 123E+00
2.950	*.00	1.0 576E+00 2.0 119E+00 2.0 123E+00 2.0 123E+00 2.0 123E+00 2.0 123E+00
2.975	*.00	1.0 637E+00 1.0 637E+00 1.0 637E+00 1.0 637E+00 1.0 637E+00 1.0 637E+00
2.980	*.00	1.0 637E+00 1.0 637E+00 1.0 637E+00 1.0 637E+00 1.0 637E+00 1.0 637E+00
3.025	*.00	1.0 637E+00 1.0 637E+00 1.0 637E+00 1.0 637E+00 1.0 637E+00 1.0 637E+00
3.075	*.00	1.0 637E+00 1.0 637E+00 1.0 637E+00 1.0 637E+00 1.0 637E+00 1.0 637E+00
3.125	*.00	1.0 637E+00 1.0 637E+00 1.0 637E+00 1.0 637E+00 1.0 637E+00 1.0 637E+00
3.175	*.00	1.0 637E+00 1.0 637E+00 1.0 637E+00 1.0 637E+00 1.0 637E+00 1.0 637E+00
3.225	*.00	1.0 637E+00 1.0 637E+00 1.0 637E+00 1.0 637E+00 1.0 637E+00 1.0 637E+00
3.275	*.00	1.0 637E+00 1.0 637E+00 1.0 637E+00 1.0 637E+00 1.0 637E+00 1.0 637E+00
3.325	*.00	1.0 637E+00 1.0 637E+00 1.0 637E+00 1.0 637E+00 1.0 637E+00 1.0 637E+00
3.375	*.00	1.0 637E+00 1.0 637E+00 1.0 637E+00 1.0 637E+00 1.0 637E+00 1.0 637E+00
3.425	*.00	1.0 637E+00 1.0 637E+00 1.0 637E+00 1.0 637E+00 1.0 637E+00 1.0 637E+00
3.475	*.00	1.0 637E+00 1.0 637E+00 1.0 637E+00 1.0 637E+00 1.0 637E+00 1.0 637E+00
3.525	*.00	1.0 637E+00 1.0 637E+00 1.0 637E+00 1.0 637E+00 1.0 637E+00 1.0 637E+00
3.575	*.00	1.0 637E+00 1.0 637E+00 1.0 637E+00 1.0 637E+00 1.0 637E+00 1.0 637E+00
3.625	*.00	1.0 637E+00 1.0 637E+00 1.0 637E+00 1.0 637E+00 1.0 637E+00 1.0 637E+00

Table A1. Listing of COMBH2O Band Model Parameter Set (Cont'd)

MEAN LINE WIDTHS IN ARAYACHITATI, HUAHU CO. NON-RESONANT SELF-SOOTCENING AT 290

Table A2. Listing of COMBCO2 Band Model Parameter Set

BAND MODEL	PARAMETERS	COMBCO2	5.00E0
ION NAME			
RESOLUTION(FWH-1)			
ALPHA(1)	• 1110E+00	RESONANT SELF-BROADENING	
ALPHA(2)	• 2730E+00	FOREIGN-GAS BROADENING(CO2)	
ALPHA(3)	0.	FOREIGN-GAS BROADENING(CO2)	
ALPHA(4)	• 7730E+00	FOREIGN-GAS BROADENING(N2)	
ALPHA(5)	• 6110E+00	FOREIGN-GAS BROADENING(O2)	
ALPHA(6)	• 4600E+02	ATOMIC WEIGHT(CAH)	
WAVE NUMBER(WN) ARRAY(C4-1)	N# = 135		
3.130E+03	3.105E+03	3.110E+03	3.115E+03
3.150E+03	3.155E+03	3.150E+03	3.150E+03
3.200E+03	3.205E+03	3.210E+03	3.215E+03
3.250E+03	3.255E+03	3.260E+03	3.275E+03
3.300E+03	3.305E+03	3.310E+03	3.320E+03
3.350E+03	3.355E+03	3.360E+03	3.375E+03
3.400E+03	3.405E+03	3.410E+03	3.420E+03
3.450E+03	3.455E+03	3.460E+03	3.475E+03
3.500E+03	3.505E+03	3.510E+03	3.525E+03
3.550E+03	3.555E+03	3.560E+03	3.575E+03
3.600E+03	3.605E+03	3.610E+03	3.625E+03
3.650E+03	3.655E+03	3.660E+03	3.675E+03
3.700E+03	3.705E+03	3.710E+03	3.725E+03
3.750E+03	3.755E+03	3.760E+03	3.775E+03
3.800E+03	3.805E+03	3.810E+03	3.825E+03
3.850E+03	3.855E+03	3.860E+03	3.875E+03
3.900E+03	3.905E+03	3.910E+03	3.925E+03
3.950E+03	3.955E+03	3.960E+03	3.975E+03
4.000E+03	4.005E+03	4.010E+03	4.025E+03
4.050E+03	4.055E+03	4.060E+03	4.075E+03
4.100E+03	4.105E+03	4.110E+03	4.125E+03
4.150E+03	4.155E+03	4.160E+03	4.175E+03
4.200E+03	4.205E+03	4.210E+03	4.225E+03
4.250E+03	4.255E+03	4.260E+03	4.275E+03
4.300E+03	4.305E+03	4.310E+03	4.325E+03
4.350E+03	4.355E+03	4.360E+03	4.375E+03
4.400E+03	4.405E+03	4.410E+03	4.425E+03
4.450E+03	4.455E+03	4.460E+03	4.475E+03
4.500E+03	4.505E+03	4.510E+03	4.525E+03
4.550E+03	4.555E+03	4.560E+03	4.575E+03
4.600E+03	4.605E+03	4.610E+03	4.625E+03
4.650E+03	4.655E+03	4.660E+03	4.675E+03
4.700E+03	4.705E+03	4.710E+03	4.725E+03
4.750E+03	4.755E+03	4.760E+03	4.775E+03
4.800E+03	4.805E+03	4.810E+03	4.825E+03
4.850E+03	4.855E+03	4.860E+03	4.875E+03
4.900E+03	4.905E+03	4.910E+03	4.925E+03
4.950E+03	4.955E+03	4.960E+03	4.975E+03
5.000E+03	5.005E+03	5.010E+03	5.025E+03
5.050E+03	5.055E+03	5.060E+03	5.075E+03
5.100E+03	5.105E+03	5.110E+03	5.125E+03
5.150E+03	5.155E+03	5.160E+03	5.175E+03
5.200E+03	5.205E+03	5.210E+03	5.225E+03
5.250E+03	5.255E+03	5.260E+03	5.275E+03
5.300E+03	5.305E+03	5.310E+03	5.325E+03
5.350E+03	5.355E+03	5.360E+03	5.375E+03
5.400E+03	5.405E+03	5.410E+03	5.425E+03
5.450E+03	5.455E+03	5.460E+03	5.475E+03
5.500E+03	5.505E+03	5.510E+03	5.525E+03
5.550E+03	5.555E+03	5.560E+03	5.575E+03
5.600E+03	5.605E+03	5.610E+03	5.625E+03
5.650E+03	5.655E+03	5.660E+03	5.675E+03
5.700E+03	5.705E+03	5.710E+03	5.725E+03
5.750E+03	5.755E+03	5.760E+03	5.775E+03
5.800E+03	5.805E+03	5.810E+03	5.825E+03
5.850E+03	5.855E+03	5.860E+03	5.875E+03
5.900E+03	5.905E+03	5.910E+03	5.925E+03
5.950E+03	5.955E+03	5.960E+03	5.975E+03
6.000E+03	6.005E+03	6.010E+03	6.025E+03
6.050E+03	6.055E+03	6.060E+03	6.075E+03
6.100E+03	6.105E+03	6.110E+03	6.125E+03
6.150E+03	6.155E+03	6.160E+03	6.175E+03
6.200E+03	6.205E+03	6.210E+03	6.225E+03
6.250E+03	6.255E+03	6.260E+03	6.275E+03
6.300E+03	6.305E+03	6.310E+03	6.325E+03
6.350E+03	6.355E+03	6.360E+03	6.375E+03
6.400E+03	6.405E+03	6.410E+03	6.425E+03
6.450E+03	6.455E+03	6.460E+03	6.475E+03
6.500E+03	6.505E+03	6.510E+03	6.525E+03
6.550E+03	6.555E+03	6.560E+03	6.575E+03
6.600E+03	6.605E+03	6.610E+03	6.625E+03
6.650E+03	6.655E+03	6.660E+03	6.675E+03
6.700E+03	6.705E+03	6.710E+03	6.725E+03
6.750E+03	6.755E+03	6.760E+03	6.775E+03
6.800E+03	6.805E+03	6.810E+03	6.825E+03
6.850E+03	6.855E+03	6.860E+03	6.875E+03
6.900E+03	6.905E+03	6.910E+03	6.925E+03
6.950E+03	6.955E+03	6.960E+03	6.975E+03
7.000E+03	7.005E+03	7.010E+03	7.025E+03
7.050E+03	7.055E+03	7.060E+03	7.075E+03
7.100E+03	7.105E+03	7.110E+03	7.125E+03
7.150E+03	7.155E+03	7.160E+03	7.175E+03
7.200E+03	7.205E+03	7.210E+03	7.225E+03
7.250E+03	7.255E+03	7.260E+03	7.275E+03
7.300E+03	7.305E+03	7.310E+03	7.325E+03
7.350E+03	7.355E+03	7.360E+03	7.375E+03
7.400E+03	7.405E+03	7.410E+03	7.425E+03
7.450E+03	7.455E+03	7.460E+03	7.475E+03
7.500E+03	7.505E+03	7.510E+03	7.525E+03
7.550E+03	7.555E+03	7.560E+03	7.575E+03
7.600E+03	7.605E+03	7.610E+03	7.625E+03
7.650E+03	7.655E+03	7.660E+03	7.675E+03
7.700E+03	7.705E+03	7.710E+03	7.725E+03
7.750E+03	7.755E+03	7.760E+03	7.775E+03
7.800E+03	7.805E+03	7.810E+03	7.825E+03
7.850E+03	7.855E+03	7.860E+03	7.875E+03
7.900E+03	7.905E+03	7.910E+03	7.925E+03
7.950E+03	7.955E+03	7.960E+03	7.975E+03
8.000E+03	8.005E+03	8.010E+03	8.025E+03
8.050E+03	8.055E+03	8.060E+03	8.075E+03
8.100E+03	8.105E+03	8.110E+03	8.125E+03
8.150E+03	8.155E+03	8.160E+03	8.175E+03
8.200E+03	8.205E+03	8.210E+03	8.225E+03
8.250E+03	8.255E+03	8.260E+03	8.275E+03
8.300E+03	8.305E+03	8.310E+03	8.325E+03
8.350E+03	8.355E+03	8.360E+03	8.375E+03
8.400E+03	8.405E+03	8.410E+03	8.425E+03
8.450E+03	8.455E+03	8.460E+03	8.475E+03
8.500E+03	8.505E+03	8.510E+03	8.525E+03
8.550E+03	8.555E+03	8.560E+03	8.575E+03
8.600E+03	8.605E+03	8.610E+03	8.625E+03
8.650E+03	8.655E+03	8.660E+03	8.675E+03
8.700E+03	8.705E+03	8.710E+03	8.725E+03
8.750E+03	8.755E+03	8.760E+03	8.775E+03
8.800E+03	8.805E+03	8.810E+03	8.825E+03
8.850E+03	8.855E+03	8.860E+03	8.875E+03
8.900E+03	8.905E+03	8.910E+03	8.925E+03
8.950E+03	8.955E+03	8.960E+03	8.975E+03
9.000E+03	9.005E+03	9.010E+03	9.025E+03
9.050E+03	9.055E+03	9.060E+03	9.075E+03
9.100E+03	9.105E+03	9.110E+03	9.125E+03
9.150E+03	9.155E+03	9.160E+03	9.175E+03
9.200E+03	9.205E+03	9.210E+03	9.225E+03
9.250E+03	9.255E+03	9.260E+03	9.275E+03
9.300E+03	9.305E+03	9.310E+03	9.325E+03
9.350E+03	9.355E+03	9.360E+03	9.375E+03
9.400E+03	9.405E+03	9.410E+03	9.425E+03
9.450E+03	9.455E+03	9.460E+03	9.475E+03
9.500E+03	9.505E+03	9.510E+03	9.525E+03
9.550E+03	9.555E+03	9.560E+03	9.575E+03
9.600E+03	9.605E+03	9.610E+03	9.625E+03
9.650E+03	9.655E+03	9.660E+03	9.675E+03
9.700E+03	9.705E+03	9.710E+03	9.725E+03
9.750E+03	9.755E+03	9.760E+03	9.775E+03
9.800E+03	9.805E+03	9.810E+03	9.825E+03
9.850E+03	9.855E+03	9.860E+03	9.875E+03
9.900E+03	9.905E+03	9.910E+03	9.925E+03
9.950E+03	9.955E+03	9.960E+03	9.975E+03
1.000E+04	1.005E+04	1.010E+04	1.015E+04

TEMPERATURE(T) ARRAY(DESK)	NT = 10	
1.000E+02	2.000E+02	3.000E+02
5.000E+02	7.000E+02	1.000E+03
7.500E+02	1.000E+03	1.500E+03
1.000E+03	2.000E+03	3.000E+03
1.500E+03	3.000E+03	4.500E+03
2.000E+03	4.000E+03	6.000E+03
2.500E+03	5.000E+03	7.500E+03
3.000E+03	6.000E+03	9.000E+03
3.500E+03	7.000E+03	1.050E+04
4.000E+03	8.000E+03	1.200E+04
4.500E+03	9.000E+03	1.350E+04
5.000E+03	1.000E+04	1.450E+04
5.500E+03	1.100E+04	1.550E+04
6.000E+03	1.200E+04	1.650E+04
6.500E+03	1.300E+04	1.750E+04
7.000E+03	1.400E+04	1.850E+04
7.500E+03	1.500E+04	1.950E+04
8.000E+03	1.600E+04	2.050E+04
8.500E+03	1.700E+04	2.150E+04
9.000E+03	1.800E+04	2.250E+04
9.500E+03	1.900E+04	2.350E+04
1.000E+04	2.000E+04	2.450E+04

ABSORPTION COEFFICIENT(K) ARRAY(CM-1/ATM)	
3.100	1.174E-10
3.105	1.198E-10
3.110	1.201E-10
3.115	1.204E-10
3.120	1.207E-10
3.125	1.210E-10
3.130	1.213E-10
3.135	1.216E-10
3.140	1.219E-10
3.145	1.222E-10
3.150	1.225E-10
3.155	1.228E-10
3.160	1.231E-10
3.165	1.234E-10
3.170	1.237E-10
3.175	1.240E-10
3.180	1.243E-10
3.185	1.246E-10

Table A2. Listing of COMBCC2 Band Model Parameter Sets Cross-Section

Table A2. Listing of COMBCO<sub>2</sub> Band Model Parameter Set (Cont'd)

Table A2. Listing of COMBCO<sub>2</sub> Band Model Parameter Set (Cont'd)

EFFECTIVE LINE DENSITY(%) ARRAY(LINES/CM-1)

Wavelength (nm)	Line Density (%)
395E-02	2.446E-01
400E-02	1.444E-01
405E-02	0.987E-01
410E-02	0.644E-01
415E-02	0.447E-01
420E-02	0.354E-01
425E-02	0.268E-01
430E-02	0.186E-01
435E-02	0.115E-01
440E-02	0.769E-02
445E-02	0.535E-02
450E-02	0.369E-02
455E-02	0.269E-02
460E-02	0.195E-02
465E-02	0.144E-02
470E-02	0.102E-02
475E-02	0.714E-03
480E-02	0.503E-03
485E-02	0.350E-03
490E-02	0.239E-03
495E-02	0.162E-03
500E-02	0.119E-03
505E-02	0.839E-04
510E-02	0.595E-04
515E-02	0.404E-04
520E-02	0.276E-04
525E-02	0.176E-04
530E-02	0.112E-04
535E-02	0.744E-05
540E-02	0.505E-05
545E-02	0.342E-05
550E-02	0.231E-05
555E-02	0.159E-05
560E-02	0.111E-05
565E-02	0.744E-06
570E-02	0.505E-06
575E-02	0.342E-06
580E-02	0.231E-06
585E-02	0.159E-06
590E-02	0.111E-06
595E-02	0.744E-07
600E-02	0.505E-07
605E-02	0.342E-07
610E-02	0.231E-07
615E-02	0.159E-07
620E-02	0.111E-07
625E-02	0.744E-08
630E-02	0.505E-08
635E-02	0.342E-08
640E-02	0.231E-08
645E-02	0.159E-08
650E-02	0.111E-08
655E-02	0.744E-09
660E-02	0.505E-09
665E-02	0.342E-09
670E-02	0.231E-09
675E-02	0.159E-09
680E-02	0.111E-09
685E-02	0.744E-10
690E-02	0.505E-10
695E-02	0.342E-10
700E-02	0.231E-10
705E-02	0.159E-10
710E-02	0.111E-10
715E-02	0.744E-11
720E-02	0.505E-11
725E-02	0.342E-11
730E-02	0.231E-11
735E-02	0.159E-11
740E-02	0.111E-11
745E-02	0.744E-12
750E-02	0.505E-12
755E-02	0.342E-12
760E-02	0.231E-12
765E-02	0.159E-12
770E-02	0.111E-12
775E-02	0.744E-13
780E-02	0.505E-13
785E-02	0.342E-13
790E-02	0.231E-13
795E-02	0.159E-13
800E-02	0.111E-13
805E-02	0.744E-14
810E-02	0.505E-14
815E-02	0.342E-14
820E-02	0.231E-14
825E-02	0.159E-14
830E-02	0.111E-14
835E-02	0.744E-15
840E-02	0.505E-15
845E-02	0.342E-15
850E-02	0.231E-15
855E-02	0.159E-15
860E-02	0.111E-15
865E-02	0.744E-16
870E-02	0.505E-16
875E-02	0.342E-16
880E-02	0.231E-16
885E-02	0.159E-16
890E-02	0.111E-16
895E-02	0.744E-17
900E-02	0.505E-17
905E-02	0.342E-17
910E-02	0.231E-17
915E-02	0.159E-17
920E-02	0.111E-17
925E-02	0.744E-18
930E-02	0.505E-18
935E-02	0.342E-18
940E-02	0.231E-18
945E-02	0.159E-18
950E-02	0.111E-18
955E-02	0.744E-19
960E-02	0.505E-19
965E-02	0.342E-19
970E-02	0.231E-19
975E-02	0.159E-19
980E-02	0.111E-19
985E-02	0.744E-20
990E-02	0.505E-20
995E-02	0.342E-20
1000E-02	0.231E-20
1005E-02	0.159E-20
1010E-02	0.111E-20
1015E-02	0.744E-21
1020E-02	0.505E-21
1025E-02	0.342E-21
1030E-02	0.231E-21
1035E-02	0.159E-21
1040E-02	0.111E-21
1045E-02	0.744E-22
1050E-02	0.505E-22
1055E-02	0.342E-22
1060E-02	0.231E-22
1065E-02	0.159E-22
1070E-02	0.111E-22
1075E-02	0.744E-23
1080E-02	0.505E-23
1085E-02	0.342E-23
1090E-02	0.231E-23
1095E-02	0.159E-23
1100E-02	0.111E-23
1105E-02	0.744E-24
1110E-02	0.505E-24
1115E-02	0.342E-24
1120E-02	0.231E-24
1125E-02	0.159E-24
1130E-02	0.111E-24
1135E-02	0.744E-25
1140E-02	0.505E-25
1145E-02	0.342E-25
1150E-02	0.231E-25
1155E-02	0.159E-25
1160E-02	0.111E-25
1165E-02	0.744E-26
1170E-02	0.505E-26
1175E-02	0.342E-26
1180E-02	0.231E-26
1185E-02	0.159E-26
1190E-02	0.111E-26
1195E-02	0.744E-27
1200E-02	0.505E-27
1205E-02	0.342E-27
1210E-02	0.231E-27
1215E-02	0.159E-27
1220E-02	0.111E-27
1225E-02	0.744E-28
1230E-02	0.505E-28
1235E-02	0.342E-28
1240E-02	0.231E-28
1245E-02	0.159E-28
1250E-02	0.111E-28
1255E-02	0.744E-29
1260E-02	0.505E-29
1265E-02	0.342E-29
1270E-02	0.231E-29
1275E-02	0.159E-29
1280E-02	0.111E-29
1285E-02	0.744E-30
1290E-02	0.505E-30
1295E-02	0.342E-30
1300E-02	0.231E-30
1305E-02	0.159E-30
1310E-02	0.111E-30
1315E-02	0.744E-31
1320E-02	0.505E-31
1325E-02	0.342E-31
1330E-02	0.231E-31
1335E-02	0.159E-31
1340E-02	0.111E-31
1345E-02	0.744E-32
1350E-02	0.505E-32
1355E-02	0.342E-32
1360E-02	0.231E-32
1365E-02	0.159E-32
1370E-02	0.111E-32
1375E-02	0.744E-33
1380E-02	0.505E-33
1385E-02	0.342E-33
1390E-02	0.231E-33
1395E-02	0.159E-33
1400E-02	0.111E-33
1405E-02	0.744E-34
1410E-02	0.505E-34
1415E-02	0.342E-34
1420E-02	0.231E-34
1425E-02	0.159E-34
1430E-02	0.111E-34
1435E-02	0.744E-35
1440E-02	0.505E-35
1445E-02	0.342E-35
1450E-02	0.231E-35
1455E-02	0.159E-35
1460E-02	0.111E-35
1465E-02	0.744E-36
1470E-02	0.505E-36
1475E-02	0.342E-36
1480E-02	0.231E-36
1485E-02	0.159E-36
1490E-02	0.111E-36
1495E-02	0.744E-37
1500E-02	0.505E-37
1505E-02	0.342E-37
1510E-02	0.231E-37
1515E-02	0.159E-37
1520E-02	0.111E-37
1525E-02	0.744E-38
1530E-02	0.505E-38
1535E-02	0.342E-38
1540E-02	0.231E-38
1545E-02	0.159E-38
1550E-02	0.111E-38
1555E-02	0.744E-39
1560E-02	0.505E-39
1565E-02	0.342E-39
1570E-02	0.231E-39
1575E-02	0.159E-39
1580E-02	0.111E-39
1585E-02	0.744E-40
1590E-02	0.505E-40
1595E-02	0.342E-40
1600E-02	0.231E-40
1605E-02	0.159E-40
1610E-02	0.111E-40
1615E-02	0.744E-41
1620E-02	0.505E-41
1625E-02	0.342E-41
1630E-02	0.231E-41
1635E-02	0.159E-41
1640E-02	0.111E-41
1645E-02	0.744E-42
1650E-02	0.505E-42
1655E-02	0.342E-42
1660E-02	0.231E-42
1665E-02	0.159E-42
1670E-02	0.111E-42
1675E-02	0.744E-43
1680E-02	0.505E-43
1685E-02	0.342E-43
1690E-02	0.231E-43
1695E-02	0.159E-43
1700E-02	0.111E-43
1705E-02	0.744E-44
1710E-02	0.505E-44
1715E-02	0.342E-44
1720E-02	0.231E-44
1725E-02	0.159E-44
1730E-02	0.111E-44
1735E-02	0.744E-45
1740E-02	0.505E-45
1745E-02	0.342E-45
1750E-02	0.231E-45
1755E-02	0.159E-45
1760E-02	0.111E-45
1765E-02	0.744E-46
1770E-02	0.505E-46
1775E-02	0.342E-46
1780E-02	0.231E-46
1785E-02	0.159E-46
1790E-02	0.111E-46
1795E-02	0.744E-47
1800E-02	0.505E-47
1805E-02	0.342E-47
1810E-02	0.231E-47
1815E-02	0.159E-47
1820E-02	0.111E-47
1825E-02	0.744E-48
1830E-02	0.505E-48
1835E-02	0.342E-48
1840E-02	0.231E-48
1845E-02	0.159E-48
1850E-02	0.111E-48
1855E-02	0.744E-49
1860E-02	0.505E-49
1865E-02	0.342E-49
1870E-02	0.231E-49
1875E-02	0.159E-49
1880E-02	0.111E-49
1885E-02	0.744E-50
1890E-02	0.505E-50
1895E-02	0.342E-50
1900E-02	0.231E-50
1905E-02	0.159E-50
1910E-02	0.111E-50
1915E-02	0.744E-51
1920E-02	0.505E-51
1925E-02	0.342E-51
1930E-02	0.231E-51
1935E-02	0.159E-51
1940E-02	0.111E-51
1945E-02	0.744E-52
1950E-02	0.505E-52
1955E-02	0.342E-52
1960E-02	0.231E-52
1965E-02	0.159E-52
1970E-02	0.111E-52
1975E-02	0.744E-53
1980E-02	0.505E-53
1985E-02	0.342E-53
1990E-02	0.231E-53
1995E-02	0.159E-53
2000E-02	0.111E-53
2005E-02	0.744E-54
2010E-02	0.505E-54
2015E-02	0.342E-54
2020E-02	0.231E-54
2025E-02	0.159E-54
2030E-02	0.111E-54
2035E-02	0.744E-55
2040E-02	0.505E-55
2045E-02	0.342E-55
2050E-02	0.231E-55
2055E-02	0.159E-55
2060E-02	0.111E-55
2065E-02	0.744E-56
2070E-02	0.505E-56
2075E-02	0.342E-56
2080E-02	0.231E-56
2085E-02	0.159E-56
2090E-02	0.111E-56
2095E-02	0.744E-57
2100E-02	0.505E-57
2105E-02	0.342E-57
2110E-02	0.231E-57
2115E-02	0.159E-57
2120E-02	0.111E-57
2125E-02	0.744E-58
2130E-02	0.505E-58
2135E-02	0.342E-58
2140E-02	0.231E-58
2145E-02	0.159E-58
2150E-02	0.111E-58
2155E-02	0.744E-59
2160E-02	0.505E-59
2165E-02	0.342E-59
2170E-02	0.231E-59
2175E-02	0.159E-59
2180E-02	0.111E-59
2185E-02	0.744E-60
2190E-02	0.505E-60
2195E-02	0.342E-60
2200E-02	0.231E-60
2205E-02	0.159E-60
2210E-02	0.111E-60
2215E-02	0.744E-61
2220E-02	0.505E-61
2225E-02	0.342E-61
2230E-02	0.231E-61
2235E-02	0.159E-61
2240E-02	0.111E-61
2245E-02	0.744E-62
2250E-02	0.505E-62
2255E-02	0.342E-62
2260E-02	0.231E-62
2265E-02	0.159E-62
2270E-02	0.111E-62
2275E-02	0.744E-63
2280E-02	0.505E-63
2285E-02	0.342E-63
2290E-02	0.231E-63
2295E-02	0.159E-63
2300E-02	0.111E-63
2305E-02	0.744E-64
2310E-02	0.505E-64
2315E-02	0.342E-64
2320E-02	0.231E-64
2325E-02	0.159E-64
2330E-02	0.111E-64
2335E-02	0.744E-65
2340E-02	0.505E-65
2345E-02	0.342E-65
2350E-02	0.231E-65
2355E-02	0.159E-65
2360E-02	0.111E-65
2365E-02	0.744E-66
2370E-02	0.505E-66
2375E-02	0.342E-66
2380E-02	0.231E-66
2385E-02	0.159E-66
2390E-02	0.111E-66
2395E-02	0.744E-67

Table A2. Listing of COMBCO<sub>2</sub> Band Model Parameter Set (Cont'd)

Table A2. Listing of COMBCO2 Band Model Parameter Set (Cont'd)

	MEAN LINE WIDTH (W)	AR-PAY(GM-1)ATH.	4444 FOR NON-RESONANT SELF-BROADENING AT 5151
3600	8.00	1.6634E+00	3.845E+00
3605	8.00	1.6634E+00	3.845E+00
3610	8.00	1.6634E+00	3.845E+00
3615	7.95	1.6634E+00	3.845E+00
3620	7.90	1.6634E+00	3.845E+00
3625	7.85	1.6634E+00	3.845E+00
3630	7.80	1.6634E+00	3.845E+00
3635	7.75	1.6634E+00	3.845E+00
3640	7.70	1.6634E+00	3.845E+00
3645	7.65	1.6634E+00	3.845E+00
3650	7.60	1.6634E+00	3.845E+00
3655	7.55	1.6634E+00	3.845E+00
3660	7.50	1.6634E+00	3.845E+00
3665	7.45	1.6634E+00	3.845E+00
3670	7.40	1.6634E+00	3.845E+00
3675	7.35	1.6634E+00	3.845E+00
3680	7.30	1.6634E+00	3.845E+00
3685	7.25	1.6634E+00	3.845E+00
3690	7.20	1.6634E+00	3.845E+00
3695	7.15	1.6634E+00	3.845E+00
3700	7.10	1.6634E+00	3.845E+00
3705	7.05	1.6634E+00	3.845E+00
3710	7.00	1.6634E+00	3.845E+00
3715	6.95	1.6634E+00	3.845E+00
3720	6.90	1.6634E+00	3.845E+00
3725	6.85	1.6634E+00	3.845E+00
3730	6.80	1.6634E+00	3.845E+00
3735	6.75	1.6634E+00	3.845E+00
3740	6.70	1.6634E+00	3.845E+00
3745	6.65	1.6634E+00	3.845E+00
3750	6.60	1.6634E+00	3.845E+00
3755	6.55	1.6634E+00	3.845E+00
3760	6.50	1.6634E+00	3.845E+00
3765	6.45	1.6634E+00	3.845E+00
3770	6.40	1.6634E+00	3.845E+00
3775	6.35	1.6634E+00	3.845E+00
3780	6.30	1.6634E+00	3.845E+00
3785	6.25	1.6634E+00	3.845E+00
3790	6.20	1.6634E+00	3.845E+00
3795	6.15	1.6634E+00	3.845E+00
3800	6.10	1.6634E+00	3.845E+00
3805	6.05	1.6634E+00	3.845E+00
3810	6.00	1.6634E+00	3.845E+00
3815	5.95	1.6634E+00	3.845E+00
3820	5.90	1.6634E+00	3.845E+00
3825	5.85	1.6634E+00	3.845E+00
3830	5.80	1.6634E+00	3.845E+00
3835	5.75	1.6634E+00	3.845E+00
3840	5.70	1.6634E+00	3.845E+00
3845	5.65	1.6634E+00	3.845E+00
3850	5.60	1.6634E+00	3.845E+00
3855	5.55	1.6634E+00	3.845E+00
3860	5.50	1.6634E+00	3.845E+00
3865	5.45	1.6634E+00	3.845E+00
3870	5.40	1.6634E+00	3.845E+00
3875	5.35	1.6634E+00	3.845E+00
3880	5.30	1.6634E+00	3.845E+00
3885	5.25	1.6634E+00	3.845E+00
3890	5.20	1.6634E+00	3.845E+00
3895	5.15	1.6634E+00	3.845E+00
3900	5.10	1.6634E+00	3.845E+00
3905	5.05	1.6634E+00	3.845E+00
3910	5.00	1.6634E+00	3.845E+00
3915	4.95	1.6634E+00	3.845E+00
3920	4.90	1.6634E+00	3.845E+00
3925	4.85	1.6634E+00	3.845E+00
3930	4.80	1.6634E+00	3.845E+00
3935	4.75	1.6634E+00	3.845E+00
3940	4.70	1.6634E+00	3.845E+00
3945	4.65	1.6634E+00	3.845E+00
3950	4.60	1.6634E+00	3.845E+00
3955	4.55	1.6634E+00	3.845E+00
3960	4.50	1.6634E+00	3.845E+00
3965	4.45	1.6634E+00	3.845E+00
3970	4.40	1.6634E+00	3.845E+00
3975	4.35	1.6634E+00	3.845E+00
3980	4.30	1.6634E+00	3.845E+00
3985	4.25	1.6634E+00	3.845E+00
3990	4.20	1.6634E+00	3.845E+00
3995	4.15	1.6634E+00	3.845E+00
4000	4.10	1.6634E+00	3.845E+00
4005	4.05	1.6634E+00	3.845E+00
4010	4.00	1.6634E+00	3.845E+00
4015	3.95	1.6634E+00	3.845E+00
4020	3.90	1.6634E+00	3.845E+00
4025	3.85	1.6634E+00	3.845E+00
4030	3.80	1.6634E+00	3.845E+00
4035	3.75	1.6634E+00	3.845E+00
4040	3.70	1.6634E+00	3.845E+00
4045	3.65	1.6634E+00	3.845E+00
4050	3.60	1.6634E+00	3.845E+00
4055	3.55	1.6634E+00	3.845E+00
4060	3.50	1.6634E+00	3.845E+00
4065	3.45	1.6634E+00	3.845E+00
4070	3.40	1.6634E+00	3.845E+00
4075	3.35	1.6634E+00	3.845E+00
4080	3.30	1.6634E+00	3.845E+00
4085	3.25	1.6634E+00	3.845E+00
4090	3.20	1.6634E+00	3.845E+00
4095	3.15	1.6634E+00	3.845E+00
4100	3.10	1.6634E+00	3.845E+00
4105	3.05	1.6634E+00	3.845E+00
4110	3.00	1.6634E+00	3.845E+00
4115	2.95	1.6634E+00	3.845E+00
4120	2.90	1.6634E+00	3.845E+00
4125	2.85	1.6634E+00	3.845E+00
4130	2.80	1.6634E+00	3.845E+00
4135	2.75	1.6634E+00	3.845E+00
4140	2.70	1.6634E+00	3.845E+00
4145	2.65	1.6634E+00	3.845E+00
4150	2.60	1.6634E+00	3.845E+00
4155	2.55	1.6634E+00	3.845E+00
4160	2.50	1.6634E+00	3.845E+00
4165	2.45	1.6634E+00	3.845E+00
4170	2.40	1.6634E+00	3.845E+00
4175	2.35	1.6634E+00	3.845E+00
4180	2.30	1.6634E+00	3.845E+00
4185	2.25	1.6634E+00	3.845E+00
4190	2.20	1.6634E+00	3.845E+00
4195	2.15	1.6634E+00	3.845E+00
4200	2.10	1.6634E+00	3.845E+00
4205	2.05	1.6634E+00	3.845E+00
4210	2.00	1.6634E+00	3.845E+00
4215	1.95	1.6634E+00	3.845E+00
4220	1.90	1.6634E+00	3.845E+00
4225	1.85	1.6634E+00	3.845E+00
4230	1.80	1.6634E+00	3.845E+00
4235	1.75	1.6634E+00	3.845E+00
4240	1.70	1.6634E+00	3.845E+00
4245	1.65	1.6634E+00	3.845E+00
4250	1.60	1.6634E+00	3.845E+00
4255	1.55	1.6634E+00	3.845E+00
4260	1.50	1.6634E+00	3.845E+00
4265	1.45	1.6634E+00	3.845E+00
4270	1.40	1.6634E+00	3.845E+00
4275	1.35	1.6634E+00	3.845E+00
4280	1.30	1.6634E+00	3.845E+00
4285	1.25	1.6634E+00	3.845E+00
4290	1.20	1.6634E+00	3.845E+00
4295	1.15	1.6634E+00	3.845E+00
4300	1.10	1.6634E+00	3.845E+00
4305	1.05	1.6634E+00	3.845E+00
4310	1.00	1.6634E+00	3.845E+00
4315	0.95	1.6634E+00	3.845E+00
4320	0.90	1.6634E+00	3.845E+00
4325	0.85	1.6634E+00	3.845E+00
4330	0.80	1.6634E+00	3.845E+00
4335	0.75	1.6634E+00	3.845E+00
4340	0.70	1.6634E+00	3.845E+00
4345	0.65	1.6634E+00	3.845E+00
4350	0.60	1.6634E+00	3.845E+00
4355	0.55	1.6634E+00	3.845E+00
4360	0.50	1.6634E+00	3.845E+00
4365	0.45	1.6634E+00	3.845E+00
4370	0.40	1.6634E+00	3.845E+00
4375	0.35	1.6634E+00	3.845E+00
4380	0.30	1.6634E+00	3.845E+00
4385	0.25	1.6634E+00	3.845E+00
4390	0.20	1.6634E+00	3.845E+00
4395	0.15	1.6634E+00	3.845E+00
4400	0.10	1.6634E+00	3.845E+00
4405	0.05	1.6634E+00	3.845E+00
4410	0.00	1.6634E+00	3.845E+00
4415	-0.05	1.6634E+00	3.845E+00
4420	-0.10	1.6634E+00	3.845E+00
4425	-0.15	1.6634E+00	3.845E+00
4430	-0.20	1.6634E+00	3.845E+00
4435	-0.25	1.6634E+00	3.845E+00
4440	-0.30	1.6634E+00	3.845E+00
4445	-0.35	1.6634E+00	3.845E+00
4450	-0.40	1.6634E+00	3.845E+00
4455	-0.45	1.6634E+00	3.845E+00
4460	-0.50	1.6634E+00	3.845E+00
4465	-0.55	1.6634E+00	3.845E+00
4470	-0.60	1.6634E+00	3.845E+00
4475	-0.65	1.6634E+00	3.845E+00
4480	-0.70	1.6634E+00	3.845E+00
4485	-0.75	1.6634E+00	3.845E+00
4490	-0.80	1.6634E+00	3.845E+00
4495	-0.85	1.6634E+00	3.845E+00
4500	-0.90	1.6634E+00	3.845E+00
4505	-0.95	1.6634E+00	3.845E+00
4510	-1.00	1.6634E+00	3.845E+00
4515	-1.05	1.6634E+00	3.845E+00
4520	-1.10	1.6634E+00	3.845E+00
4525	-1.15	1.6634E+00	3.845E+00
4530	-1.20	1.6634E+00	3.845E+00
4535	-1.25	1.6634E+00	3.845E+00
4540	-1.30	1.6634E+00	3.845E+00
4545	-1.35	1.6634E+00	3.845E+00
4550	-1.40	1.6634E+00	3.845E+00
4555	-1.45	1.6634E+00	3.845E+00
4560	-1.50	1.6634E+00	3.845E+00
4565	-1.55	1.6634E+00	3.845E+00
4570	-1.60	1.6634E+00	3.845E+00
4575	-1.65	1.6634E+00	3.845E+00
4580	-1.70	1.6634E+00	3.845E+00
4585	-1.75	1.6634E+00	3.845E+00
4590	-1.80	1.6634E+00	3.845E+00
4595	-1.85	1.6634E+00	3.845E+00
4600	-1.90	1.6634E+00	3.845E+00
4605	-1.95	1.6634E+00	3.845E+00
4610	-2.00	1.6634E+00	3.845E+00
4615	-2.05	1.6634E+00	3.845E+00
4620	-2.10	1.6634E+00	3.845E+00
4625	-2.15	1.6634E+00	3.845E+00
4630	-2.20	1.6634E+00	3.845E+00
4635	-2.25	1.6634E+00	3.845E+00
4640	-2.30	1.6634E+00	3.845E+00

## LABORATORY OPERATIONS

The Laboratory Operations of The Aerospace Corporation is conducting experimental and theoretical investigations necessary for the evaluation and application of scientific advances to new military concepts and systems. Versatility and flexibility have been developed to a high degree by the laboratory personnel in dealing with the many problems encountered in the nation's rapidly developing space and missile systems. Expertise in the latest scientific developments is vital to the accomplishment of tasks related to these problems. The laboratories that contribute to this research are:

Aerophysics Laboratory: Launch and reentry aerodynamics, heat transfer, reentry physics, chemical kinetics, structural mechanics, flight dynamics, atmospheric pollution, and high-power gas lasers.

Chemistry and Physics Laboratory: Atmospheric reactions and atmospheric optics, chemical reactions in polluted atmospheres, chemical reactions of excited species in rocket plumes, chemical thermodynamics, plasma and laser-induced reactions, laser chemistry, propulsion chemistry, space vacuum and radiation effects on materials, lubrication and surface phenomena, photo-sensitive materials and sensors, high precision laser ranging, and the application of physics and chemistry to problems of law enforcement and biomedicine.

Electronics Research Laboratory: Electromagnetic theory, devices, and propagation phenomena, including plasma electromagnetics; quantum electronics, lasers, and electro-optics; communication sciences, applied electronics, semiconducting, superconducting, and crystal device physics, optical and acoustical imaging; atmospheric pollution; millimeter wave and far-infrared technology.

Materials Sciences Laboratory: Development of new materials; metal matrix composites and new forms of carbon; test and evaluation of graphite and ceramics in reentry; spacecraft materials and electronic components in nuclear weapons environment; application of fracture mechanics to stress corrosion and fatigue-induced fractures in structural metals.

Space Physics Laboratory: Atmospheric and ionospheric physics, radiation from the atmosphere, density and composition of the atmosphere, aurorae and airglow; magnetospheric physics, cosmic rays, generation and propagation of plasma waves in the magnetosphere; solar physics, studies of solar magnetic fields; space astronomy, x-ray astronomy; the effects of nuclear explosions, magnetic storms, and solar activity on the earth's atmosphere, ionosphere, and magnetosphere; the effects of optical, electromagnetic, and particulate radiations in space on space systems.

THE AEROSPACE CORPORATION  
El Segundo, California